frontiers | Frontiers in Earth Science

TYPE Original Research
PUBLISHED 22 June 2023
DOI 10.3389/feart.2023.1221485

OPEN ACCESS

EDITED BY
Basilios Tsikouras,
Universiti Brunei Darussalam, Brunei

REVIEWED BY
Georgia Pe-Piper,
Saint Mary's University, Canada
Sergey Khromykh,
V. S. Sobolev Institute of Geology and Mineralogy (RAS), Russia

*CORRESPONDENCE
Alongkot Fanka,
alongkot.f@chula.ac.th

RECEIVED 12 May 2023
ACCEPTED 07 June 2023
PUBLISHED 22 June 2023

CITATION
Fanka A and Tadthai J (2023), Petrology and geochemistry of Li-bearing pegmatites and related granitic rocks in southern Thailand: implications for petrogenesis and lithium potential in Thailand.
Front. Earth Sci. 11:1221485.
doi: 10.3389/feart.2023.1221485

Petrology and geochemistry of Li-bearing pegmatites and related granitic rocks in southern Thailand: implications for petrogenesis and lithium potential in Thailand

Alongkot Fanka[1]* and Jaruphichaya Tadthai[2]

[1]Department of Geology, Applied Mineral and Petrology Special Task Force for Activating Research (AMP STAR), Faculty of Science, Chulalongkorn University, Bangkok, Thailand, [2]Department of Geology, Faculty of Science, Chulalongkorn University, Bangkok, Thailand

Lithium (Li) can be found in many minerals, including lepidolite. Lepidolite is found in pegmatite-related tin deposits in the Phang Nga area in southern Thailand. According to their field occurrence, petrography, mineral chemistry, and whole-rock geochemistry, the Li-bearing pegmatites and the granitic rocks in the study area can be linked to tin deposits in southern Thailand as part of the SE Asian tin belt. The Li-bearing pegmatites are characterized by an abundance of lepidolite, K-feldspar, plagioclase, and quartz with some accessory minerals of fluorite, cassiterite, apatite, monazite, and beryl. The granitic rocks show various compositions, including porphyritic biotite–muscovite granite, biotite granite, and muscovite—tourmaline granite with different proportions of K-feldspar, plagioclase, quartz, biotite, muscovite, and tourmaline. Whole-rock geochemistry indicates that both the Li-bearing pegmatites and granitic rocks have a close relationship rooted in their peraluminous S-type granite affinity. The Li-bearing pegmatites evolved from highly fractionated S-type granitic rocks comparable with the Western Belt Granite of Thailand. The enrichment of large-ion lithophile elements (e.g., Rb and K) and the depletion of Ba, Nb, and Ti together with similar rare Earth element patterns reflect the collisional setting indicating the Sibumasu–West Burma and West Burma—Indo-Burma collisions during the Cretaceous to the Eocene. The crystallization pressure—temperature conditions of these rocks were 3.49–4.25 kbar and 622°C–675°C, respectively, with an emplacement depth of 13–15 km. The Li-bearing pegmatites had a relatively high average Li grade compared with those of other Li-bearing pegmatites in the world.

KEYWORDS

lithium, lepidolite, pegmatite, granite, Thailand, tin belt, Southeast Asia (SE Asia)

1 Introduction

Nowadays, lithium (Li) has become an important element in many industries (e.g., energy storage), especially in the energy industry. Li can be found in many minerals, such as spodumene, lepidolite, amblygonite, petalite in granitic rocks, and pegmatites (Averill and Olson, 1978; Gao et al., 2020; Zhang et al., 2020; Groves et al., 2022). These Li-bearing rocks

evolved from highly fractionated granites (Cerny, 1991a; Cerny, 1991b; Muller et al., 2022; Shen et al., 2022) that migrated from parental granite to rare-metal-rich pegmatites, including Li-bearing pegmatites. Lepidolite pegmatites are well-defined Li sources in several deposits in the world, such as the Alakha deposits in Russia (Annikova et al., 2016), the Zavitinskoye deposits in Russia (Seltmann et al., 2010; Melentiev et al., 2022), and the La Vi, Quang Ngai deposits in Vietnam (Hien-Dinh et al., 2017).

Lepidolite pegmatite and related granitic rocks (Cobbing et al., 1992; Nakapadungrat and Putthapiban, 1992; Charusiri et al., 1993) have been discovered in the tin deposits in the Phang Nga area, southern Thailand (Figure 1) (Suthakorn, 1992; Nakapadungrat and Maneenai, 1993). These rocks comprise the SE Asia tin belt (Cobbing et al., 1992; Nakapadungrat and Putthapiban, 1992; Charusiri et al., 1993), which is associated with various types of tin deposits (DMR, 2009), such as argillic dissemination, quartz–cassiterite–wolframite vein swarm, and pegmatite types (Gocht and Pluhar, 1982; Nakapadungrat and Maneenai, 1993; DMR, 2009). Moreover, granitic rocks related to tin deposits are distributed in many areas along the Western Belt Granite (WBG) of Thailand, such as Chiang Mai, the Thai–Burma border in Kanchanaburi, Ratchaburi together with the Phang Nga–Phuket area, and other areas in SE Asia (e.g., Dhawai, Burma; Nakapadungrat and Putthapiban, 1992; Cobbing et al., 1992; Li et al., 2019).

Although there are some reports about tin deposits related to lepidolite pegmatite in Thailand (Suthakorn, 1992; Nakapadungrat and Maneenai, 1993), detailed studies on the petrology and geochemistry of lepidolite pegmatite and related granitic rocks associated with tin deposits in Phang Nga area, southern Thailand, have never made. Therefore, this research aims to provide the petrology, mineral chemistry, and geochemistry of lepidolite pegmatite and related granitic rocks in the Phang Nga tin field, southern Thailand, to understand the petrogenesis, tectonic setting, and Li potential in Thailand and the SE Asia tin belt.

2 Geological background

Granitic rocks widely distributed throughout Thailand and SE Asia (Cobbing et al., 1992; Nakapadungrat and Putthapiban, 1992; Charusiri et al., 1993) are classified into three main belts: the Eastern

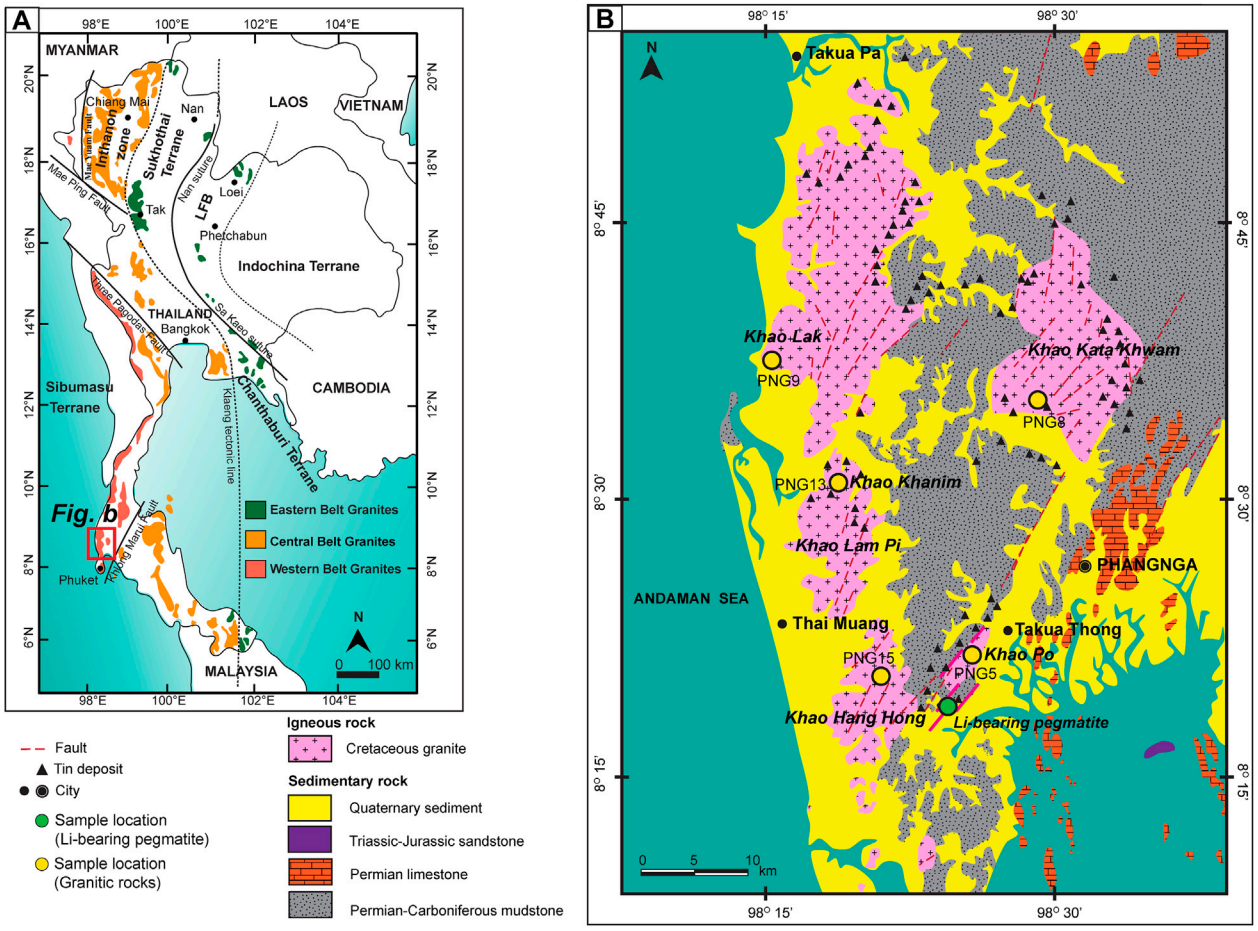

FIGURE 1
(A) Index map of Thailand showing the distribution of three main granitic belts (Nakapadungrat and Putthapiban, 1992; Charusiri et al., 1993) and main tectonic terranes (Charusiri et al., 2002; Sone and Metcalfe, 2008; Sone et al., 2012; Zaw et al., 2014). **(B)** Geological map of the Phang Nga area, southern Thailand, together with the sample locations (DMR, 1985).

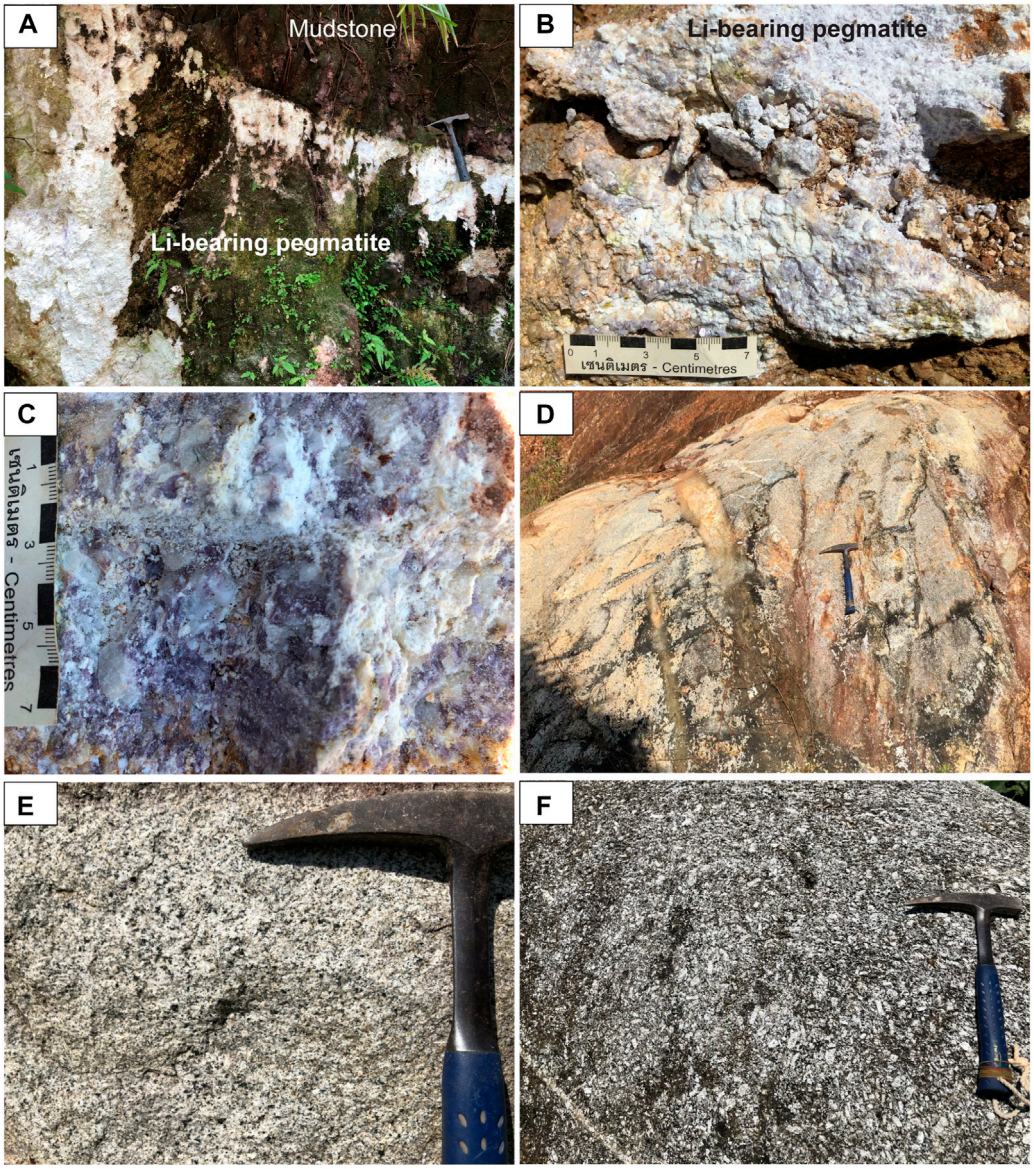

FIGURE 2
(A) Outcrop exposure of the Li-bearing pegmatites cut into the host rock of mudstone; **(B,C)** lepidolite in the Li-bearing pegmatite; **(D–F)** granitic rocks associated with tin deposits exposed in the Phang Nga area, southern Thailand.

Belt Granite, the Central Belt Granite, and WBG in a mainly N–S trend (Figure 1A). The WBG is the main exposed belt in western Thailand near the Thailand–Burma border and extending to western peninsular Thailand (Cobbing et al., 1992; Nakapadungrat and Putthapiban, 1992; Charusiri et al., 1993) (Figure 1A). It has been termed the Western Tin Belt or Tin Province (Cobbing et al., 1986), which includes the Phang Nga area, southern Thailand (Figure 1B) (Nakapadungrat and Maneenai, 1993). In the Phang Nga area (Figure 1B), granitic rocks are exposed in several locations, such as in the Khao Lak, Khao Khanim, Khao Lam Pi, Khao Kata Khwam, Khao Hang Hong, and Khao Po areas (DMR, 1985). These granitic are of various types, such as biotite granite, biotite–muscovite granite, muscovite–tourmaline granite, and pegmatite (Nakapadungrat and Maneenai, 1993). These granitic rocks are associated with tin deposits (Suwimonprecha, 1989; Nakapadungrat and Maneenai, 1993) distributed in several tin fields (Figure 1B).

The granites of the Phang Nga area are exposed along the western coast and central part of the Phang Nga were intruded into Permo-Carboniferous sedimentary rocks, Permian limestone, and Triassic–Jurassic sedimentary rocks and were covered by Quaternary sediment (DMR, 1985) (Figure 1B). The Permo-Carboniferous sedimentary rocks widely distributed in the Phang Nga area, especially the western part of the study area (Figure 1B), comprise mainly pebbly mudstone, laminated sandstone, siltstone, and shale (Tantiwanit et al., 1983; DMR, 1985). The Permian limestone, exposed in the central part of the area and extending to the southern part, is a gray bedded to

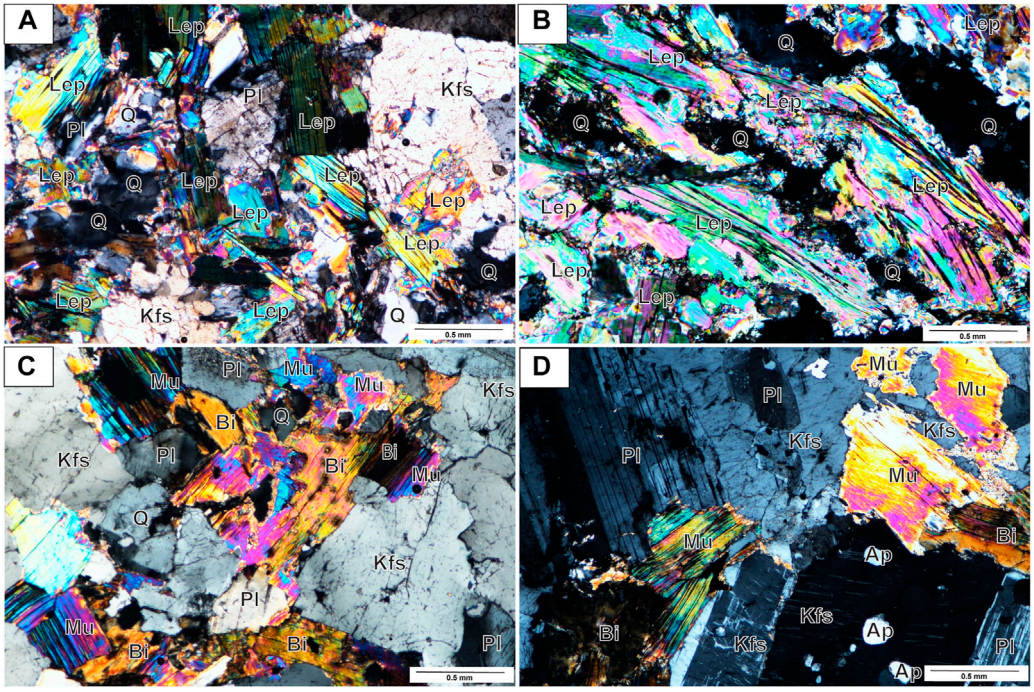

FIGURE 3
Photomicrograph under cross-polarization (XPL) of the **(A,B)** Li-bearing pegmatites and **(C,D)** related granitic rocks in the Phang Nga area, southern Thailand. Abbreviations: Lep (lepidolite); Q (quartz); Kfs (K-feldspar); Pl (plagioclase); Bi (biotite); Mu (muscovite); Ap (apatite).

massive fossiliferous limestone (DMR, 1985). Triassic–Jurassic sedimentary rocks, found only in the southern part of the area, include mainly sandstone, conglomerate, siltstone, and argillaceous limestone (DMR, 1985).

3 Analytical methods

Six representative Li-bearing pegmatites and five related granitic rocks exposed in the Phang Nga area, southern Thailand (Figure 1), were collected from the least weathered zone to study their petrography, mineral chemistry, and whole-rock geochemistry. Representative granitic rocks were collected from main granitic exposures, including Khao Po (PNG5), Khao Hang Hong (PNG15), Khao Khanim (PNG13), Khao Lak (PNG9), and Khao Kata Khwam (PNG8) (Figure 1B).

All rock samples were prepared as polished thin sections using grinding powder and diamond paste at the Department of Geology, Faculty of Science, Chulalongkorn University. A Nikon polarized light microscope was used to observe petrographic characteristics.

The mineral chemical study was conducted using an electron probe micro-analyzer (EPMA; model JEOL JXA-8100) installed at the Department of Geology, Faculty of Science, Chulalongkorn University. The conditions for the analysis were set at 15 kV and about 2 μA using a focused beam spot (1 μm). Mineral and pure oxide standards were used for calibration at the same conditions with automatic ZAF correction and the analyses are reported as oxide weight percentages. The Li_2O content of lepidolite was calculated after Tischendorf et al. (1997).

Representative samples were prepared using a disc mill and were fused to be fused beads for whole-rock geochemical analysis. The major and minor oxides of the samples were analyzed using an X-ray fluorescence spectrometer (Bruker model AXS S-4 Pioneer) based at the Department of Geology, Faculty of Science, Chulalongkorn University. The major and minor oxides, including SiO_2, TiO_2, Al_2O_3, FeO_{total}, MnO, MgO, CaO, Na_2O, K_2O, and P_2O_5, were analyzed along with international rock standards for calibration. Loss on ignition was also conducted by measuring weight loss after heating at 1,050°C for 3 h in a furnace. In addition, trace and rare Earth element (REE) compositions were analyzed through inductively coupled plasma-mass spectrometry (ICP-MS) at ALS, Vientiane, Laos PDR with detection limits from 0.0004 ppm to 0.01%.

4 Results

4.1 Field occurrence and petrographic description

In the Phang Nga area, one of the main tin fields of Thailand, Li-bearing pegmatites are found as lepidolite pegmatite dikes related to tin deposits near Khao Po in the Takua Thong tin field (Figure 1B). Li-bearing pegmatites with a width ranging from 1 to 10 m are oriented along the NE–SW trend and cut into Carboniferous–Permian mudstone (Figure 2A). These pegmatites appear to have a similar trend with that of the Khlong Marui Fault zone (Figure 1A).

TABLE 1 Representative EPMA analyses of lepidolite in the Li-bearing pegmatites in the Phang Nga area, Southern Thailand.

Analysis no.	C6-3LP4-1	c7-3LP1-2	C9-2LP1-2	C9-2LP2-1	C9-2LP3-1	C9-2LP3-2	C9-2LP4-2	C9-2LP6-1	C9-2LP6-2	C5-2LP7-2	C5-2LP9-1	C5-2LP10-2	C1-3LP1-2	C1-3LP4-1	C1-3LP4-2	C1-3LP7-1	C4-1LP3-2	C4-1LP4-2	C4-1LP6-1	C4-1LP6-2
Mineral name	Lep	Lep	Lep	Lep	Lep	Lep	Lep	Lep	Lep	Lep	Lep	Lep	Lep	Lep	Lep	Lep	Lep	Lep	Lep	Lep
SiO2	51.13	51.64	51.18	50.57	51.15	50.75	51.13	50.77	50.84	50.25	50.54	50.51	51.10	51.36	51.88	50.35	51.32	51.15	51.03	50.80
Al2O3	26.17	26.38	27.19	26.76	26.23	27.20	27.16	27.30	27.43	27.90	27.30	26.39	27.02	25.51	25.84	27.51	26.83	26.59	26.25	28.16
TiO2	0.03	0.08	0.04	0.07	0.00	0.00	0.00	0.04	0.02	0.08	0.03	0.00	0.00	0.03	0.08	0.00	0.08	0.07	0.19	0.09
FeO	0.05	0.21	0.19	0.08	0.09	0.09	0.01	0.04	0.03	0.04	0.11	0.13	0.00	0.01	0.03	0.01	0.11	0.02	0.25	0.10
MnO	1.25	1.40	1.19	0.46	0.60	0.59	0.21	0.27	0.23	0.63	1.11	2.24	1.11	1.05	1.04	0.01	1.42	0.56	1.01	1.01
MgO	0.03	0.01	0.01	0.02	0.01	0.00	0.00	0.01	0.01	0.00	0.00	0.00	0.02	0.00	0.08	0.00	0.01	0.00	0.05	0.00
CaO	0.00	0.01	0.00	0.03	0.02	0.00	0.00	0.00	0.04	0.01	0.00	0.01	0.00	0.01	0.02	0.32	0.00	0.00	0.00	0.00
Na2O	0.19	0.18	0.38	0.44	0.47	0.46	0.68	0.63	0.66	0.12	0.46	0.29	0.20	0.31	0.20	0.28	0.33	0.50	0.12	0.38
K2O	10.56	10.67	10.28	10.73	10.58	10.57	10.18	10.61	10.75	10.99	10.10	10.14	10.33	10.26	10.37	10.08	10.29	10.31	10.73	10.22
Li2O[a]	5.12	5.27	5.13	4.96	5.12	5.01	5.12	5.02	5.03	4.86	4.95	4.94	5.11	5.18	5.34	4.89	5.17	5.12	5.09	5.02
Total	94.53	95.83	95.58	94.10	94.27	94.66	94.48	94.68	95.01	94.89	94.58	94.65	94.89	93.71	94.88	93.45	95.56	94.33	94.72	95.77
22 (O)																				
Si	6.739	6.724	6.667	6.691	6.748	6.669	6.700	6.665	6.656	6.603	6.649	6.680	6.692	6.806	6.789	6.664	6.690	6.728	6.720	6.596
Al	4.065	4.047	4.173	4.172	4.076	4.212	4.194	4.223	4.231	4.320	4.232	4.112	4.170	3.983	3.984	4.291	4.122	4.121	4.072	4.309
Ti	0.003	0.007	0.004	0.007	0.000	0.000	0.000	0.003	0.001	0.008	0.003	0.000	0.000	0.003	0.008	0.000	0.007	0.007	0.018	0.009
Li[a]	2.712	2.756	2.688	2.637	2.718	2.646	2.696	2.647	2.649	2.569	2.616	2.626	2.690	2.762	2.807	2.603	2.711	2.709	2.695	2.622
Fe2+	0.005	0.023	0.020	0.008	0.010	0.009	0.001	0.004	0.003	0.004	0.012	0.014	0.000	0.001	0.003	0.001	0.012	0.003	0.027	0.011
Mn	0.139	0.155	0.131	0.052	0.067	0.066	0.024	0.030	0.025	0.070	0.124	0.251	0.123	0.117	0.116	0.001	0.157	0.062	0.113	0.111
Mg	0.006	0.001	0.001	0.003	0.001	0.001	0.000	0.002	0.002	0.001	0.000	0.001	0.004	0.000	0.016	0.000	0.002	0.000	0.009	0.000
Ca	0.000	0.001	0.001	0.004	0.003	0.000	0.000	0.000	0.005	0.001	0.000	0.002	0.000	0.002	0.002	0.045	0.000	0.000	0.000	0.000
Na	0.049	0.046	0.095	0.113	0.121	0.116	0.172	0.161	0.166	0.030	0.116	0.073	0.050	0.080	0.052	0.072	0.084	0.128	0.031	0.096
K	1.775	1.771	1.707	1.810	1.779	1.772	1.701	1.776	1.794	1.842	1.695	1.711	1.725	1.733	1.729	1.701	1.710	1.729	1.802	1.692
Total	15.494	15.532	15.488	15.496	15.522	15.491	15.488	15.511	15.532	15.449	15.446	15.469	15.455	15.487	15.506	15.379	15.495	15.488	15.489	15.445

[a]Calculated after Tischendorf et al. (1997).

10.3389/feart.2023.1221485

TABLE 2 Representative EPMA analyses of biotite in the granitic rocks in the Phang Nga area, southern Thailand.

Analysis No.	PNG15Bi1-1	PNG15Bi1-2	PNG15Bi2-1	PNG15Bi2-2	PNG15Bi3-1	PNG15Bi3-2	PNG9Bi1-1	PNG9Bi1-2	PNG9Bi2-1
SiO2	34.36	34.83	34.23	34.47	34.09	33.66	34.39	33.97	33.35
Al2O3	17.88	17.64	18.33	18.37	17.56	17.81	17.85	18.16	17.75
TiO2	2.28	2.35	2.36	2.30	2.50	2.45	2.82	2.95	2.85
Cr2O3	0.00	0.00	0.02	0.00	0.00	0.03	0.04	0.00	0.05
FeOt	24.16	25.68	25.23	24.50	25.71	25.09	24.54	24.89	24.74
MnO	0.64	0.64	0.71	0.66	0.69	0.66	0.30	0.34	0.38
MgO	5.61	5.59	5.55	5.73	5.39	5.43	5.76	5.37	5.74
CaO	0.00	0.00	0.00	0.00	0.03	0.00	0.00	0.00	0.00
Na2O	0.07	0.06	0.12	0.05	0.14	0.10	0.05	0.05	0.08
K2O	0.02	0.02	0.00	0.00	0.02	0.01	0.01	0.00	0.00
Total	85.02	86.80	86.54	86.08	86.13	85.25	85.75	85.73	84.93
22 (O)									
Si	5.687	5.685	5.599	5.639	5.627	5.600	5.646	5.594	5.557
Al	3.486	3.394	3.534	3.540	3.416	3.491	3.453	3.523	3.485
Ti	0.284	0.288	0.290	0.283	0.311	0.307	0.348	0.365	0.357
Cr	0.000	0.000	0.002	0.000	0.000	0.004	0.006	0.000	0.006
Fe2+	3.343	3.505	3.451	3.351	3.548	3.489	3.368	3.425	3.446
Mn	0.090	0.088	0.098	0.091	0.097	0.094	0.042	0.048	0.053
Mg	1.383	1.358	1.351	1.397	1.325	1.345	1.407	1.318	1.423
Ca	0.000	0.000	0.000	0.000	0.006	0.000	0.000	0.000	0.000
Na	0.023	0.019	0.038	0.015	0.045	0.031	0.014	0.016	0.024
K	0.004	0.004	0.000	0.001	0.004	0.003	0.002	0.001	0.000
Total	14.300	14.341	14.362	14.316	14.379	14.363	14.286	14.289	14.353
Temperature (oC)*	622.5	624.3	625.7	622.0	637.1	635.3	657.5	664.0	661.6

(Continued on following page)

10.3389/feart.2023.1221485

TABLE 2 (*Continued*) Representative EPMA analyses of biotite in the granitic rocks in the Phang Nga area, southern Thailand.

Analysis No.	PNG15Bi1-1	PNG15Bi1-2	PNG15Bi2-1	PNG15Bi2-2	PNG15Bi3-1	PNG15Bi3-2	PNG9Bi1-1	PNG9Bi1-2	PNG9Bi2-1
Pressure (kbar)**	4.0	3.8	4.2	4.2	3.8	4.0	3.9	4.1	4.0
Depth (km)	15	14	15	15	14	15	14	15	15
PNG9Bi2-2	PNG8Bi1-1	PNG8Bi1-2	PNG8Bi2-1	PNG8Bi2-2	PNG8Bi3-1	PNG8Bit3-2	PNG8Bi4-1	PNG8Bi4-2	
32.96	34.03	34.57	34.90	34.46	34.34	34.23	34.21	35.00	
18.06	17.46	17.37	17.67	17.31	17.66	17.40	17.05	17.15	
2.93	3.09	3.16	2.98	2.99	3.07	3.09	2.83	2.68	
0.03	0.06	0.03	0.01	0.08	0.01	0.04	0.01	0.00	
25.58	24.50	24.73	25.53	24.87	25.13	24.26	25.47	25.33	
0.34	0.40	0.37	0.38	0.39	0.38	0.43	0.41	0.39	
5.05	5.86	5.77	5.68	5.74	5.62	5.64	5.88	5.77	
0.00	0.00	0.00	0.00	0.00	0.00	0.00	0.10	0.04	
0.09	0.00	0.08	0.09	0.09	0.04	0.10	0.10	0.05	
0.02	0.00	0.03	0.03	0.01	0.00	0.00	0.02	0.00	
85.06	85.40	86.10	87.25	85.95	86.26	85.18	86.09	86.40	
5.510	5.621	5.664	5.656	5.663	5.627	5.660	5.639	5.723	
3.558	3.398	3.353	3.374	3.352	3.409	3.390	3.313	3.305	
0.369	0.384	0.389	0.363	0.369	0.378	0.384	0.351	0.330	
0.004	0.008	0.004	0.001	0.010	0.001	0.006	0.002	0.000	
3.575	3.384	3.387	3.459	3.417	3.442	3.353	3.510	3.463	
0.048	0.055	0.052	0.053	0.055	0.053	0.060	0.057	0.053	
1.257	1.443	1.407	1.370	1.405	1.372	1.390	1.444	1.405	
0.000	0.000	0.000	0.000	0.000	0.000	0.000	0.018	0.006	
0.030	0.000	0.024	0.027	0.029	0.013	0.033	0.033	0.016	
0.005	0.000	0.005	0.005	0.003	0.001	0.000	0.005	0.000	
14.357	14.293	14.285	14.309	14.302	14.297	14.275	14.372	14.303	
664.7	673.5	675.0	663.6	666.9	670.3	673.1	658.9	648.4	

(Continued on following page)

10.3389/feart.2023.1221485

TABLE 2 (*Continued*) Representative EPMA analyses of biotite in the granitic rocks in the Phang Nga area, southern Thailand.

PNG9Bi2-2	PNG8Bi1-1	PNG8Bi1-2	PNG8Bi2-1	PNG8Bi2-2	PNG8Bi3-1	PNG8Bit3-2	PNG8Bi4-1	PNG8Bi4-2
4.3	3.8	3.6	3.7	3.6	3.8	3.7	3.5	3.5
15	14	13	13	13	14	14	13	13

[a]Calculated after Henry et al. (2005).
[b]Calculated after Uchida et al. (2007).

TABLE 3 Representative EPMA analyses of feldspars in the Li-bearing pegmatites and granitic rocks in the Phang Nga area, Southern Thailand.

Rock-Type	Li-bearing pegmatite									
Analysis No.	C7-3F3-1	C7-3F4-1	C7-3F5-1	C7-3F7-2	C5-2F1-1	C1-3F2-2	C3-1F3-2	C1-3F6-1	C4-1F1-1	C4-1F1-2
SiO2	67.24	67.15	67.41	66.51	67.99	67.60	67.30	68.43	67.72	68.09
Al2O3	19.67	19.62	19.71	20.22	19.63	19.79	19.92	19.30	20.30	20.02
TiO2	0.00	0.00	0.00	0.00	0.00	0.00	0.00	0.00	0.02	0.03
FeO	0.04	0.00	0.03	0.00	0.00	0.00	0.00	0.01	0.00	0.00
MnO	0.01	0.00	0.02	0.00	0.01	0.02	0.00	0.02	0.04	0.02
MgO	0.00	0.01	0.00	0.00	0.00	0.01	0.00	0.00	0.00	0.01
CaO	0.43	0.70	0.29	1.05	0.37	0.28	0.39	0.24	0.78	0.70
Na2O	11.81	11.46	11.84	11.57	11.31	11.38	11.41	11.44	11.18	11.27
K2O	0.10	0.12	0.06	0.10	0.08	0.09	0.11	0.10	0.08	0.05
Total	99.30	99.05	99.36	99.45	99.38	99.17	99.12	99.54	100.12	100.19

(Continued on following page)

10.3389/feart.2023.1221485

TABLE 3 (*Continued*) Representative EPMA analyses of feldspars in the Li-bearing pegmatites and granitic rocks in the Phang Nga area, Southern Thailand.

Rock-Type	Li-bearing pegmatite									
Analysis No.	C7-3F3-1	C7-3F4-1	C7-3F5-1	C7-3F7-2	C5-2F1-1	C1-3F2-2	C3-1F3-2	C1-3F6-1	C4-1F1-1	C4-1F1-2
8 (O)										
Si	2.968	2.969	2.971	2.937	2.987	2.978	2.969	3.001	2.959	2.971
Al	1.023	1.022	1.024	1.052	1.016	1.027	1.036	0.998	1.045	1.030
Ti	0.000	0.000	0.000	0.000	0.000	0.000	0.000	0.000	0.001	0.001
Fe2+	0.001	0.000	0.001	0.000	0.000	0.000	0.000	0.001	0.000	0.000
Mn	0.000	0.000	0.001	0.000	0.000	0.001	0.000	0.001	0.001	0.001
Mg	0.000	0.001	0.000	0.000	0.000	0.001	0.000	0.000	0.000	0.000
Ca	0.020	0.033	0.014	0.050	0.017	0.013	0.018	0.011	0.037	0.033
Na	1.010	0.982	1.011	0.990	0.962	0.971	0.975	0.972	0.946	0.953
K	0.006	0.007	0.004	0.006	0.004	0.005	0.006	0.005	0.004	0.003
Total	5.028	5.014	5.025	5.035	4.988	4.996	5.004	4.989	4.993	4.991
An%	0.02	0.03	0.01	0.05	0.02	0.01	0.02	0.01	0.04	0.03
Ab%	0.97	0.96	0.98	0.95	0.98	0.98	0.98	0.98	0.96	0.96
Or%	0.01	0.01	0.00	0.01	0.00	0.01	0.01	0.01	0.00	0.00

Li-bearing pegmatite										
C9-2F1-1	C9-2F1-2	PNG13F1-2	PNG13F2-2	PNG13F3-2	PNG15F1-2	PNG15F2-1	PNG9F2-1	PNG8F1-2	PNG8F1-1	PNG8F2-1
65.08	66.03	67.11	64.16	67.47	66.25	66.86	66.80	66.10	65.72	65.47
18.72	18.39	19.61	21.67	20.13	19.92	20.13	20.05	20.21	17.72	16.66
0.15	0.14	0.00	0.00	0.00	0.00	0.00	0.00	0.02	0.04	0.00
0.21	0.22	0.02	0.00	0.04	0.02	0.02	0.05	0.09	0.03	0.08
0.05	0.07	0.00	0.00	0.01	0.00	0.03	0.00	0.01	0.00	0.00
0.01	0.00	0.01	0.00	0.00	0.00	0.00	0.00	0.02	0.00	0.00
0.00	0.00	2.22	4.47	0.97	1.93	2.18	1.70	1.74	0.04	0.00
0.30	0.20	9.93	8.64	10.58	11.48	11.45	11.98	11.65	0.75	1.03
15.21	14.72	0.24	0.28	0.09	0.03	0.00	0.01	0.02	16.34	16.10

(Continued on following page)

10.3389/feart.2023.1221485

TABLE 3 (*Continued*) Representative EPMA analyses of feldspars in the Li-bearing pegmatites and granitic rocks in the Phang Nga area, Southern Thailand.

Li-bearing pegmatite										
C9-2F1-1	C9-2F1-2	PNG13F1-2	PNG13F2-2	PNG13F3-2	PNG15F1-2	PNG15F2-1	PNG9F2-1	PNG8F1-2	PNG8F1-1	PNG8F2-1
99.75	99.76	99.15	99.26	99.33	99.63	100.72	100.60	99.86	100.63	99.36
2.997	3.026	2.965	2.851	2.966	2.929	2.926	2.928	2.918	3.021	3.050
1.016	0.993	1.021	1.135	1.043	1.038	1.038	1.035	1.051	0.960	0.914
0.005	0.005	0.000	0.000	0.000	0.000	0.000	0.000	0.001	0.001	0.000
0.008	0.008	0.001	0.000	0.002	0.001	0.001	0.002	0.003	0.001	0.003
0.002	0.003	0.000	0.000	0.000	0.000	0.001	0.000	0.000	0.000	0.000
0.001	0.000	0.001	0.000	0.000	0.000	0.000	0.000	0.001	0.000	0.000
0.000	0.000	0.105	0.213	0.046	0.092	0.102	0.080	0.082	0.002	0.000
0.027	0.018	0.850	0.744	0.902	0.984	0.971	1.017	0.996	0.067	0.093
0.893	0.860	0.013	0.016	0.005	0.002	0.000	0.001	0.001	0.958	0.956
4.949	4.912	4.956	4.961	4.965	5.045	5.040	5.063	5.054	5.010	5.017
0.00	0.00	0.11	0.22	0.05	0.08	0.10	0.07	0.08	0.00	0.00
0.03	0.02	0.88	0.76	0.95	0.91	0.90	0.93	0.92	0.06	0.09
0.97	0.98	0.01	0.02	0.01	0.00	0.00	0.00	0.00	0.93	0.91

10.3389/feart.2023.1221485

TABLE 4 Representative EPMA analyses of cassiterite in the Li-bearing pegmatites in the Phang Nga area, Southern Thailand.

Rock type	Li-bearing pegmatite											
Analysis no	C1-3Cas1-1	C1-3Cas1-2	C1-3Cas1-3	C1-3Cas2-1	C1-3Cas2-2	C1-3Cas2-3	C4-1Cas2-1	C4-1Cas2-2	C4-1Cas2-3	C4-1Cas4-1	C4-1Cas4-2	C4-1Cas4-3
WO3	0.09	0.02	0.01	0.00	0.07	0.05	0.08	0.05	0.00	0.00	0.00	0.00
SiO2	0.26	0.25	0.24	0.28	0.41	0.26	0.30	0.50	0.22	0.45	0.32	0.27
TiO2	0.00	0.00	0.00	0.00	0.50	0.21	0.00	0.08	0.00	0.31	0.15	0.00
SnO2	98.29	97.59	98.57	98.15	97.38	98.29	97.21	97.19	98.53	97.04	97.33	98.03
UO2	0.00	0.01	0.06	0.00	0.00	0.00	0.00	0.00	0.00	0.01	0.00	0.00
ThO2	0.00	0.00	0.03	0.00	0.02	0.00	0.00	0.00	0.01	0.00	0.00	0.04
ZrO2	0.15	0.11	0.04	0.06	0.37	0.14	0.07	0.54	0.04	0.27	0.29	0.07
HfO2	0.00	0.00	0.00	0.00	0.06	0.18	0.03	0.00	0.07	0.10	0.09	0.04
Sc2O3	0.00	0.00	0.00	0.00	0.00	0.00	0.00	0.00	0.00	0.09	0.00	0.00
Al2O3	0.05	0.00	0.01	0.03	0.17	0.05	0.04	0.05	0.01	0.09	0.08	0.01
MnO	0.03	0.07	0.02	0.00	0.59	0.37	0.13	1.14	0.00	0.83	0.84	0.00
MgO	0.00	0.03	0.04	0.04	0.00	0.01	0.00	0.09	0.00	0.00	0.00	0.01
CaO	0.82	0.76	0.80	0.76	0.79	0.82	0.78	0.75	0.80	0.77	0.80	0.80
PbO	0.07	0.02	0.00	0.01	0.07	0.01	0.00	0.04	0.00	0.00	0.01	0.00
Nb2O5	0.14	0.00	0.20	0.00	0.00	0.13	0.06	0.09	0.00	0.29	0.17	0.00
Ta2O5	0.92	0.31	0.89	0.47	0.72	0.71	0.58	0.13	0.10	0.66	0.81	0.00
Total	100.82	99.17	100.90	99.79	101.15	101.22	99.27	100.65	99.78	100.89	100.90	99.28
2 (O)												
W	0.001	0.000	0.000	0.000	0.000	0.000	0.001	0.000	0.000	0.000	0.000	0.000
Si	0.006	0.006	0.006	0.007	0.010	0.006	0.007	0.012	0.005	0.011	0.008	0.007
Ti	0.000	0.000	0.000	0.000	0.009	0.004	0.000	0.001	0.000	0.006	0.003	0.000
Sn	0.969	0.978	0.971	0.977	0.949	0.963	0.972	0.952	0.982	0.948	0.955	0.981
U	0.000	0.000	0.000	0.000	0.000	0.000	0.000	0.000	0.000	0.000	0.000	0.000
Th	0.000	0.000	0.000	0.000	0.000	0.000	0.000	0.000	0.000	0.000	0.000	0.000
Zr	0.002	0.001	0.001	0.001	0.004	0.002	0.001	0.007	0.001	0.003	0.003	0.001
Hf	0.000	0.000	0.000	0.000	0.000	0.001	0.000	0.000	0.001	0.001	0.001	0.000
Sc	0.000	0.000	0.000	0.000	0.000	0.000	0.000	0.000	0.000	0.002	0.000	0.000
Al	0.001	0.000	0.000	0.001	0.005	0.002	0.001	0.001	0.000	0.003	0.002	0.000
Mn	0.001	0.001	0.000	0.000	0.012	0.008	0.003	0.024	0.000	0.017	0.017	0.000
Mg	0.000	0.001	0.001	0.001	0.000	0.000	0.000	0.003	0.000	0.000	0.000	0.001
Ca	0.022	0.020	0.021	0.020	0.021	0.022	0.021	0.020	0.021	0.020	0.021	0.022
Pb	0.000	0.000	0.000	0.000	0.000	0.000	0.000	0.000	0.000	0.000	0.000	0.000
Nb	0.002	0.000	0.002	0.000	0.000	0.001	0.001	0.001	0.000	0.003	0.002	0.000
Ta	0.006	0.002	0.006	0.003	0.005	0.005	0.004	0.001	0.001	0.004	0.005	0.000
Total	1.010	1.011	1.010	1.010	1.017	1.014	1.011	1.023	1.011	1.018	1.018	1.011

TABLE 5 Representative EPMA analyses of ilmenite and titanite in the granitic rocks in the Phang Nga area, Southern Thailand.

Rock type	Granitic rock							Granitic rock					
Analysis no.	PNG13Op2-1	PNG15Op2-2	PNG15Op3-1	PNG9Op2-2	PNG9Op3-1	PNG8Op1-2	PNG8Op3-2	PNG1Tit1-2	PNG1Tit2-2	PNG8Tit1-1	PNG8Tit1-2	PNG8Tit1-3	PNG8Tit1-4
Mineral name	Ilmenite	Ilmenite	Ilmenite	Ilmenite	Ilmenite	Ilmenite	Ilmenite	Titanite	Titanite	Titanite	Titanite	Titanite	Titanite
SiO2	0.04	0.07	0.09	0.07	0.03	0.07	0.05	30.63	30.39	30.57	30.43	30.85	30.22
Al2O3	0.00	0.02	0.02	0.00	0.02	0.02	0.00	1.77	1.89	5.77	5.65	5.73	5.47
TiO2	51.95	51.96	51.90	51.57	52.88	51.82	51.68	36.66	36.91	33.43	33.84	34.00	34.70
Cr2O3	0.00	0.04	0.03	0.00	0.04	0.01	0.00	0.00	0.00	0.00	0.00	0.06	0.00
FeO	46.34	46.83	45.99	47.23	46.47	47.36	46.83	1.61	1.86	0.85	0.71	0.81	0.85
MnO	0.71	0.74	1.10	0.83	0.74	0.63	0.91	0.20	0.19	0.12	0.12	0.15	0.17
MgO	0.01	0.01	0.02	0.03	0.02	0.01	0.02	0.01	0.04	0.02	0.00	0.00	0.02
CaO	0.00	0.00	0.00	0.00	0.00	0.00	0.00	28.20	27.79	28.28	28.36	28.34	27.75
Na2O	0.00	0.02	0.02	0.00	0.01	0.01	0.00	0.00	0.00	0.04	0.01	0.00	0.02
K2O	0.00	0.00	0.03	0.00	0.00	0.00	0.00	0.00	0.00	0.01	0.02	0.04	0.04
Total	99.05	99.68	99.18	99.72	100.20	99.93	99.49	99.09	99.08	99.08	99.13	99.97	99.22
apfu	3(O)							5(O)					
Si	0.001	0.002	0.002	0.002	0.001	0.002	0.001	1.013	1.005	1.001	0.996	1.000	0.988
Al	0.000	0.001	0.001	0.000	0.000	0.001	0.000	0.069	0.074	0.222	0.218	0.219	0.211
Ti	0.997	0.992	0.994	0.986	1.001	0.988	0.990	0.911	0.918	0.822	0.832	0.829	0.853
Cr	0.000	0.001	0.001	0.000	0.001	0.000	0.000	0.000	0.000	0.000	0.000	0.002	0.000
Fe2+	0.989	0.994	0.980	1.005	0.978	1.005	0.998	0.044	0.052	0.023	0.019	0.022	0.023
Mn	0.015	0.016	0.024	0.018	0.016	0.013	0.020	0.006	0.005	0.003	0.003	0.004	0.005
Mg	0.000	0.000	0.001	0.001	0.001	0.000	0.001	0.000	0.002	0.001	0.000	0.000	0.001
Ca	0.000	0.000	0.000	0.000	0.000	0.000	0.000	0.999	0.984	0.991	0.994	0.984	0.972
Na	0.000	0.001	0.001	0.000	0.001	0.001	0.000	0.000	0.000	0.003	0.001	0.000	0.001
K	0.000	0.000	0.001	0.000	0.000	0.000	0.000	0.000	0.000	0.001	0.001	0.002	0.002
Total	2.002	2.006	2.004	2.012	1.998	2.010	2.009	3.042	3.040	3.067	3.064	3.061	3.055

10.3389/feart.2023.1221485

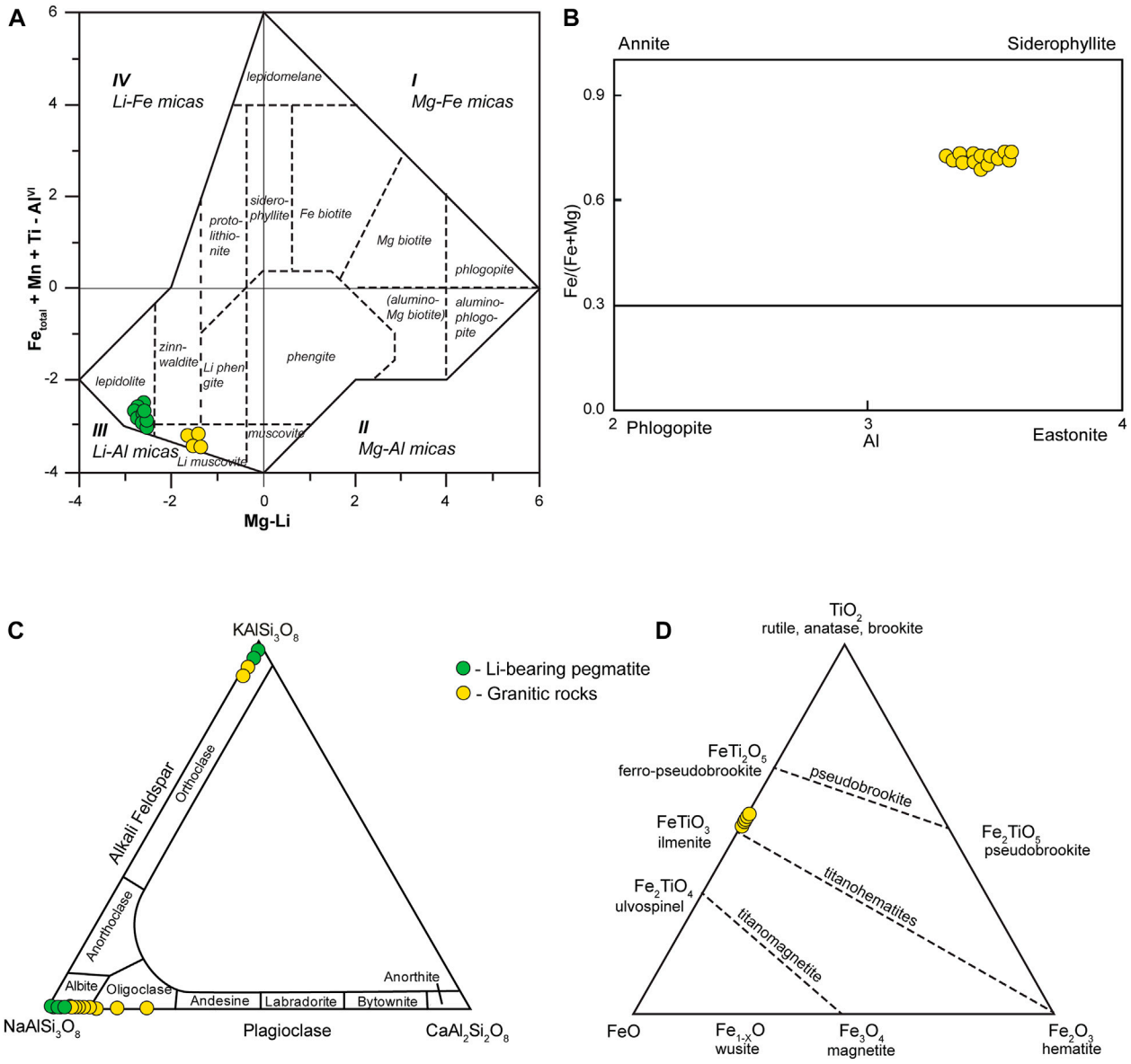

FIGURE 4
Mineral chemistry plots of **(A)** lepidolite compositions (after Tischendorf et al., 1997); **(B)** biotite compositions (after Morimoto et al., 1988); **(C)** feldspar compositions (after Smith and Brown, 1974); **(D)** ilmenite (after Deer et al., 2013).

Representative samples from the pegmatites were collected from the least weathered Li-bearing pegmatites. The Li-bearing pegmatites show phaneritic with some porphyritic textures (Figures 2B, C) with coarse grains (1–2 cm). The main mineral assemblages (Figures 3A, B) include lepidolite, K-feldspar, plagioclase, and quartz with or without accessory minerals of fluorite, cassiterite, apatite, monazite, and beryl. The main minerals in the Li-bearing pegmatites comprised lepidolite at about 20%–30%, feldspar at 30%–40%, and quartz at 20%–40%, with 1%–5% other accessory minerals. The lepidolite was clearly subhedral micaceous with grain sizes that ranged from 0.2 mm to 1 cm. Meanwhile, subhedral and anhedral K-feldspars (0.5 mm–2 cm) were commonly presented as phenocrysts producing the seriate porphyritic texture of the pegmatite. Subhedral and anhedral plagioclase crystals with albite twinning were 0.5 mm–1 cm in size. Subhedral fluorite (0.3 mm–1 cm), anhedral beryl (0.2–0.5 mm), subhedral monazite (0.2–0.5 mm), and cassiterite (<0.1–0.2 mm) were present in some samples.

In the study area, the Li-bearing pegmatites were associated with granitic rocks (Figures 2D–F) in the Phang Nga area (Figure 1B) in the WBG (Nakapadungrat and Putthapiban, 1992; Charusiri et al., 1993), SE Asia tin belt (Cobbling et al., 1992).

The above granitic rocks were characterized by porphyritic biotite–muscovite granite (with some biotite granite) and muscovite–tourmaline granite (Figure 2). The porphyritic biotite–muscovite granites were distributed in all granitic exposures in the study area (Figure 1B). Porphyritic textures with feldspar phenocrysts were very common (Figure 2F). Some

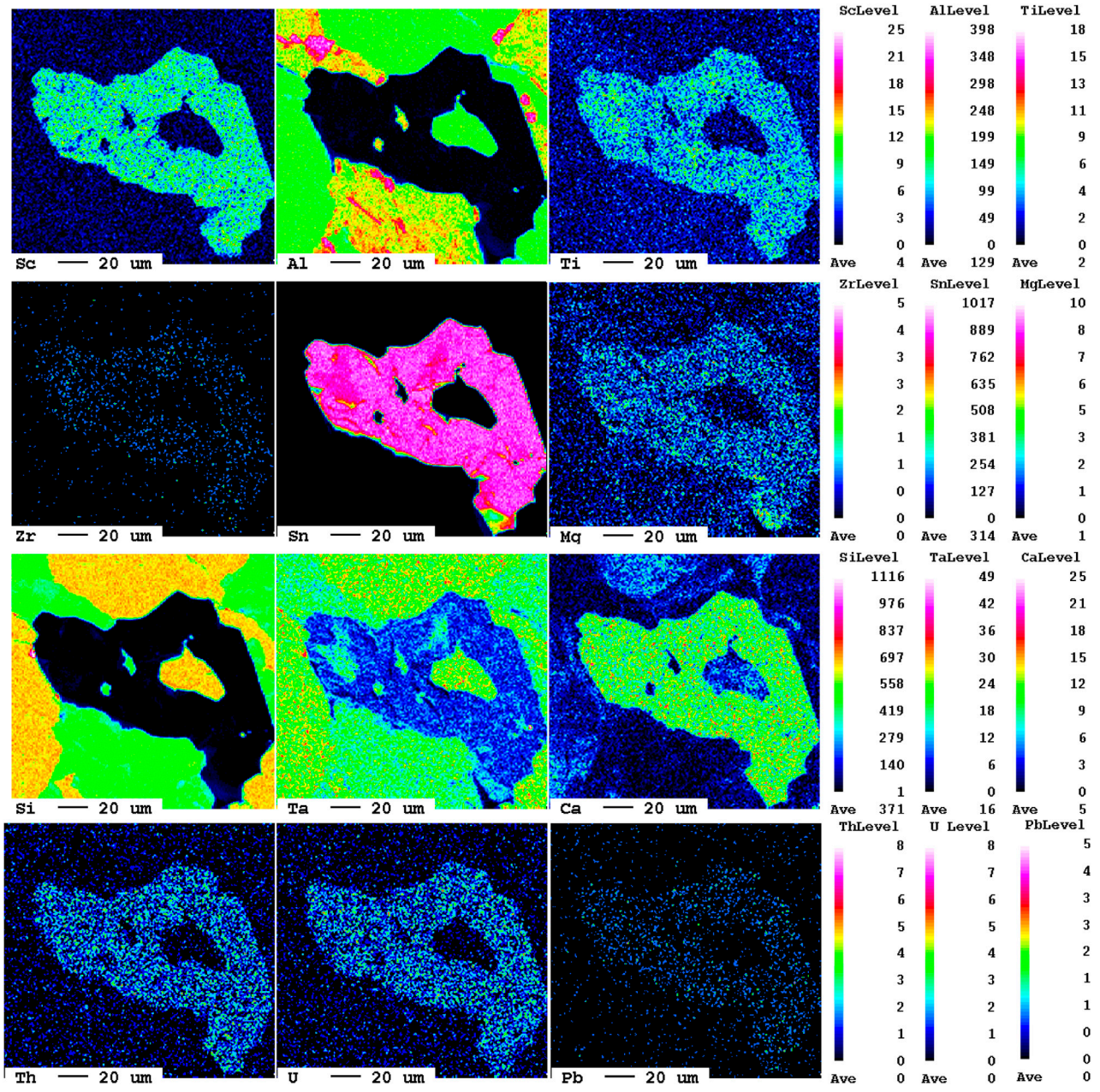

FIGURE 5
Composition mapping of cassiterite in the Li-bearing pegmatites in the Phang Nga area, Southern Thailand.

equigranular texture with medium grains was also found in the muscovite-rich granite (Figure 2E). These granitic rocks were composed mainly of K-feldspar, plagioclase, quartz, biotite, muscovite with accessory minerals of opaque minerals, apatite, zircon, titanite, monazite, and tourmaline.

In terms of microscopic characters (Figures 3C, D), subhedral to anhedral K-feldspars were found as phenocrysts (5 mm–5 cm) and groundmass (0.5–3 mm). A gride twin was clearly observed in microcline. Perthitic textures of alkali feldspar were also found. Subhedral to anhedral plagioclase that ranged in size from 0.3 to 3 mm were clearly observed with significant albite twins and sometimes Carlsbad–albite twins. Anhedral quartz with a size of 0.5–1 mm was a typical composition. Myrmekitic texture was commonly found in quartz. Biotite was very common in the granitic rocks with typical subhedral to anhedral crystals (0.5–4 mm). The biotite showed a flaky texture with different proportions from 5% to 20% in the different granitic exposures. Subhedral to anhedral muscovite (0.5–3 mm) with a flaky texture was also common in the granitic rocks. For the other accessory minerals, suhedral to subhedral titanite (0.5–1 mm), subhedral to anhedral apatite (0.2–0.5 mm), subhedral zircon (0.1–0.3 mm), subhedral to subhedral monazite (0.2–0.5 mm), and subhedral tourmaline (0.4–1 mm) were commonly found in the granitic rocks. In addition, anhedral opaque minerals (0.1–0.3 mm) were also present as accessory minerals.

TABLE 6 Representative whole-rock geochemistry of Li-bearing pegmatites and granitic rocks in the Phang Nga area, Southern Thailand.

Sample no.	Li-bearing pegmatite						Granitic rocks				
	PNG-C1	PNG-C4	PNG-C5	PNG-C6	PNG-C7	PNG-C9	PNG5	PNG8	PNG9	PNG13	PNG15
Oxides (wt%) by XRF											
SiO2	68.16	66.45	66.01	69.29	67.45	70.00	72.48	70.31	73.93	74.93	73.84
TiO2	0.00	0.02	0.02	0.03	0.02	0.02	0.50	0.58	0.32	0.17	0.15
Al2O3	20.72	22.59	21.74	19.96	21.61	19.28	13.00	13.59	12.91	12.64	13.53
FeOt	0.12	0.18	0.48	0.14	0.13	0.12	2.55	3.07	1.94	1.15	1.22
MnO	0.30	0.52	0.80	0.27	0.27	0.24	0.04	0.05	0.05	0.03	0.04
MgO	0.03	0.05	0.08	0.02	0.02	0.05	0.68	0.95	0.46	0.17	0.20
CaO	0.60	0.26	0.21	0.52	0.74	0.94	1.30	2.18	1.23	1.02	0.98
Na2O	3.95	3.52	2.60	4.44	4.32	5.63	2.16	2.28	2.40	2.84	2.84
K2O	4.29	4.61	5.44	3.22	3.97	2.18	5.38	5.48	5.51	5.28	5.61
P2O5	0.19	0.08	0.08	0.03	0.06	0.04	0.12	0.19	0.08	0.07	0.07
LOI	1.82	1.86	2.15	1.99	2.05	1.38	1.47	1.39	1.17	1.11	1.42
Total	100.18	100.14	99.61	99.91	100.64	99.87	99.69	100.07	99.99	99.40	99.90
Li2O	1.40	0.62	1.10	1.00	1.12	0.37	0.02	0.04	0.03	0.04	0.04
Li (%)	0.65	0.29	0.51	0.46	0.52	0.17	0.01	0.02	0.01	0.02	0.0176
Trace and REE (ppm) by ICP-MS											
Li	6,520	2,900	5,090	4,640	5,200	1700	96.1	182.5	125	183	176
B	111	72	124	61	64	38	—	—	—	—	—
Ba	<2	16	7	2	3	11	530	710	245	103	112
Be	400	210	186	139.5	430	300	5.11	6.04	9.72	7.9	10.9
Cu	<20	<20	<20	<20	<20	<20	5.39	6.2	3.75	1.62	3.38
Ni	30	10	10	10	10	20	6.68	6.77	3.68	0.99	1.31
Sr	<20	<20	<20	<20	<20	<20	86.7	123	60.5	31.5	37.2
V	<1	6	2	<1	1	1	27	46	13.4	3.7	3.9
Zn	10	70	60	20	40	40	49.8	54.5	57.3	45.4	50.5
Bi	0.1	0.3	0.6	0.7	1	0.5	0.751	0.64	2.79	4.13	4.94
Ce	4.2	4.3	6.9	4.1	2.8	1.3	85.4	145	290	121.5	105
Co	0.9	0.7	0.8	0.6	0.5	0.6	123	62.7	49.3	44.8	48.8
Cs	329	80.4	242	284	325	105.5	31.7	33.5	63.5	101.5	34.8
Dy	2.61	1.14	1.32	1.22	0.78	0.15	6.9	7.96	12.1	6.34	5.71
Er	0.48	0.38	0.43	0.44	0.13	0.1	3.7	4.47	5.06	2.76	2.31
Eu	<0.03	<0.03	0.03	<0.03	<0.03	<0.03	0.939	1.24	0.838	0.319	0.325
Ga	92.6	108.5	90.7	78.5	104.5	63.2	18.1	17.9	23.5	24.1	25.4
Gd	1.01	1.05	0.63	0.91	0.94	0.18	7.56	9.58	16.5	8.06	7.18
Ge	7.8	5.6	6.1	7.2	8	7.5	0.13	0.19	0.29	0.15	0.16
Ho	0.16	0.15	0.15	0.16	0.09	0.02	1.24	1.505	1.94	1.01	0.878
La	2.01	1.81	3.21	1.83	1.5	0.6	54.8	89.7	148.5	57.2	50.8

(Continued on following page)

TABLE 6 (*Continued*) Representative whole-rock geochemistry of Li-bearing pegmatites and granitic rocks in the Phang Nga area, Southern Thailand.

Sample no.	Li-bearing pegmatite						Granitic rocks				
	PNG-C1	PNG-C4	PNG-C5	PNG-C6	PNG-C7	PNG-C9	PNG5	PNG8	PNG9	PNG13	PNG15
Lu	0.09	0.07	0.08	0.07	<0.05	<0.05	0.435	0.552	0.528	0.298	0.264
Nb	55.7	52.8	70.4	30.1	44.4	37.6	23.3	22.4	31.4	36.1	40.4
Nd	1.71	2.12	2.62	1.81	1.37	0.4	44.1	68	117	49	42.3
Pb	5.4	10.3	4.5	11	9.3	8.1	49.3	41.8	72.1	61.3	66
Pr	0.45	0.46	0.69	0.5	0.42	0.15	11.6	18.6	34.9	13.4	11.7
Rb	4,520	2,570	4,550	3,510	4,370	1,560	372	366	564	629	662
Sm	1.2	1.03	1.89	1.09	1.92	0.48	8.78	12	23.4	10.7	9.48
Sn	734	987	580	651	573	1,210	8.18	6.45	23.7	35.9	32.7
Ta	232	96	221	64.8	126	32.3	4.11	2.97	5.61	7.11	7.71
Tb	0.28	0.24	0.26	0.24	0.19	0.02	1.1	1.345	2.22	1.145	1.075
Th	13	9.7	8.4	10.1	7.2	4.4	42.9	49.3	86.3	68.7	58.4
Tl	15.1	8.42	15.35	13.05	14.65	5.06	1.985	1.82	2.81	3.48	3.77
Tm	0.11	0.06	0.06	0.06	0.03	0.01	0.487	0.596	0.659	0.358	0.298
U	11.7	3.8	8.3	4.8	4.5	1.6	8.22	6.96	16.75	30.2	31.2
W	22.7	8.1	25.1	18.8	27.9	9.9	1,010	500	310	390	430
Y	19.4	7.6	9.4	12.7	6	2.1	34.5	42.1	55.5	29.2	22.9
Yb	1.27	0.56	0.74	0.78	0.22	0.07	3.07	3.73	3.82	2.14	1.875

[a]by XRF.
[b]by ICP-MS.

4.2 Mineral chemistry

The chemistry of selected minerals in the Li-bearing pegmatites and host granites was analyzed. These minerals include lepidolite, biotite, feldspar, cassiterite, ilmenite, and titanite. The analytical results are summarized in Tables 1–5.

4.2.1 Lepidolite

The compositions of lepidolite, an essential mineral in the Li-bearing pegmatite, are summarized in Table 1. These compositions showed high SiO_2 (50.25–51.88 wt%), Al_2O_3 (25.51–28.16 wt%), and K_2O (10.08–10.99 wt%) contents with low MnO (0.01–2.24 wt%) and MgO (0.00–0.08 wt%) contents. The Li_2O contents ranged from 4.86 to 5.34 wt%, as calculated after Tischendorf et al. (1997). The lepidolite compositions clearly plot in the lepidolite field (Figure 4A) of Tischendorf et al. (2001).

4.2.2 Biotite

Biotite, commonly found in the granitic rocks in this study, showed an aluminum content that ranged from 3.31 to 3.56 pfu (17.05–18.38 wt% Al_2O_3) with the TiO_2 and FeO_{total} contents of 2.28–3.16 wt% and 24.46–25.71 wt%, respectively. Biotite was not present in the Li-bearing pegmatite. This biotite in the granitic rocks was classified into the annite–siderophyllite end-member following the classification of Deer et al. (1966) (Figure 4B). The mineral chemistry of the biotite is summarized in Table 2.

4.2.3 Feldspar

The mineral chemistry of feldspar, including K-feldspar and plagioclase, is presented in Table 3. The composition plots in the feldspar ternary diagram are shown in Figure 4C. The K-feldspar in the Li-bearing pegmatites showed higher orthoclase contents ($Or_{97–98}$) than those of the granitic rocks ($Or_{91–93}$) (Figure 4C). For the plagioclase compositions, the plagioclases in the granitic rocks were albite to oligoclase ($An_{0–22}$), whereas those in the Li-bearing pegmatites were in the albite range ($An_{0–5}$) (Figure 4C).

4.2.4 Cassiterite

Cassiterite was found in the Li-bearing pegmatites as one of the traditional tin deposits in southern Thailand (Figure 1B). The mineral chemistry of cassiterite in the Li-bearing pegmatites is summarized in Table 4. The cassiterite consists predominantly of SnO_2 (97.04–98.57 wt%), with some SiO_2 (0.22–0.50 wt%), ZrO_2 (0.04–0.54 wt%), Sc_2O_3 (0.00–0.09 wt%), CaO (0.75–0.82 wt%), MgO (0.00–0.09 wt%), MnO (0.00–1.14 wt%), and Ta_2O_5 (0.00–0.92 wt%). The representative compositions of cassiterite are shown in Figure 5.

4.2.5 Ilmenite

Ilmenite was a dominant opaque mineral in the studied granitic rocks. Representative ilmenites were analyzed for their mineral chemistry (as summarized in Table 5). They comprised mainly

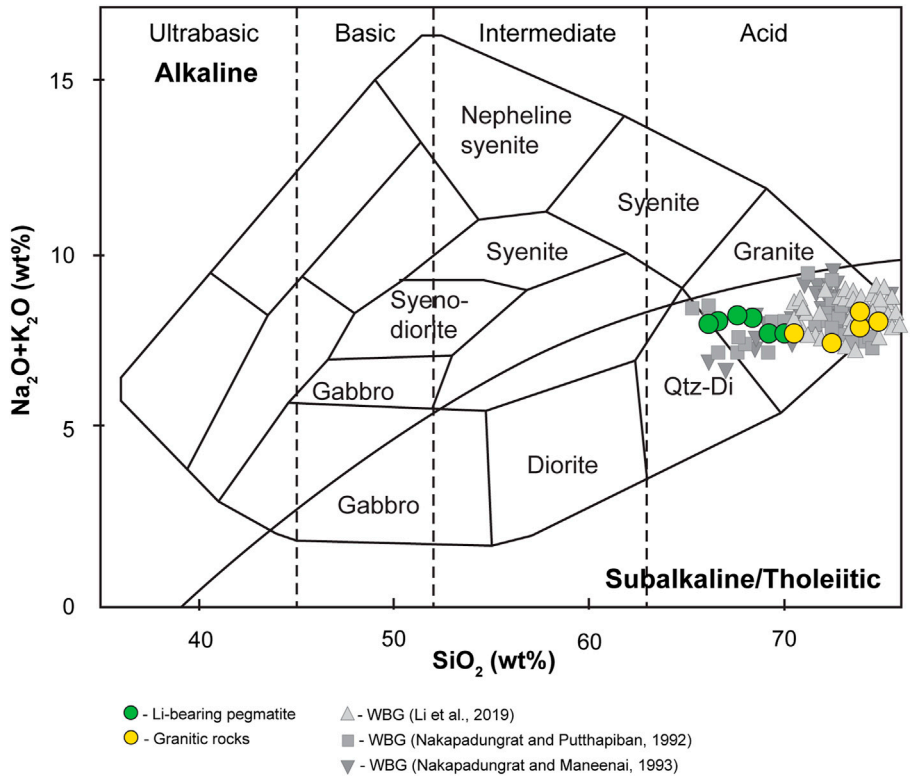

FIGURE 6
TAS discrimination diagram (Cox et al., 1979) of the Li-bearing pegmatites and related granitic rocks in the Phang Nga area, Southern Thailand, together with the granitic rocks in WGB.

TiO_2 that ranged from 51.57 to 52.88 wt% and FeO_{total} that ranged from 45.99 to 47.36 wt%, with low contents of Al_2O_3 (0.00–0.02 wt %), MnO (0.63–1.10 wt%), and MgO (0.01–0.03 wt%). Solid-solution end-member plots of these ilmenites are clearly defined in Figure 4D.

4.2.6 Titanite

Titanite or sphene, an accessory mineral in the studied granitic rocks, showed high SiO_2 (30.22–30.85 wt%), Al_2O_3 (33.43–36.91 wt %), and CaO (27.75–28.36 wt%) contents, with less TiO_2 (1.77–5.77 wt%), FeO (0.71–1.86 wt%), and MnO (0.12–0.20 wt %). The analytical data for titanite are presented in Table 5.

4.3 Whole-rock geochemistry

Whole-rock major and trace compositions of the Li-bearing pegmatites and granitic rocks are summarized in Table 6. The Li-bearing pegmatites and granitic rocks had varying SiO_2 contents from 66.01 to 74.93 wt%, where the Li-bearing pegmatites had a slightly lower SiO_2 content (66.01–70.00 wt%) than that of the granitic rocks (70.31–74.93 wt%). Generally, the Li-bearing pegmatites showed lower FeO_{total} (0.12–0.48 wt%), MgO (0.12–0.48 wt%), and CaO (0.21–0.94 wt%) contents than those of the granitic rocks (1.15–3.07 wt% FeO_{total}, 0.17–0.95 wt% MgO, and 0.98–2.18 wt% CaO). Meanwhile, the Li-bearing pegmatites exhibited higher Al_2O_3 (19.28–22.59 wt%), MnO (0.24–0.80 wt%), and Na_2O (2.60–5.63 wt%) contents than those of the granitic rocks (12.64–13.59 wt% Al_2O_3, 0.03–0.05 wt % MnO, and 2.16–2.84 wt% Na_2O). Moreover, both the Li-bearing pegmatites and the granitic rocks showed high contents of Na_2O+ K_2O, which ranged from 7.66 to 8.29 wt% and 7.55 to 8.46 wt%, respectively. The total alkali–silica (TAS) plot of SiO_2 and total alkali (Cox et al., 1979) revealed that all samples of the Li-bearing pegmatites and the granitic rocks were in the granite field (Figure 6).

Chondrite-normalized spider diagrams (Figure 7A) of both Li-bearing pegmatites and granites show the marked enrichment of large-ion lithophile elements (LILEs), such as Rb and K, with the depletion of Ba, Nb, and Ti. Chondrite-normalized REE patterns (Figure 7B) of both groups show similar patterns that are slightly high in light REEs (LREEs). Moreover, the chondrite-normalized spider diagrams and REE patterns of both groups are clearly comparable with those of typical S-type granitic rocks in WBG reported by Li et al. (2019). In addition, the chondrite-normalized La/Yb of the Li-bearing pegmatites ranges from 1.14 to 6.15, whereas that of the granitic rocks ranges from 12.80 to 27.88. Meanwhile, the $(La/Sm)_N$ ratio of the Li-bearing pegmatites and granitic rocks are 0.50–1.13 and 3.45–4.83, respectively. For the total REEs (∑REE), the granitic rocks (124–282 ppm) also feature values higher than those of the Li-bearing pegmatites (37–80 ppm).

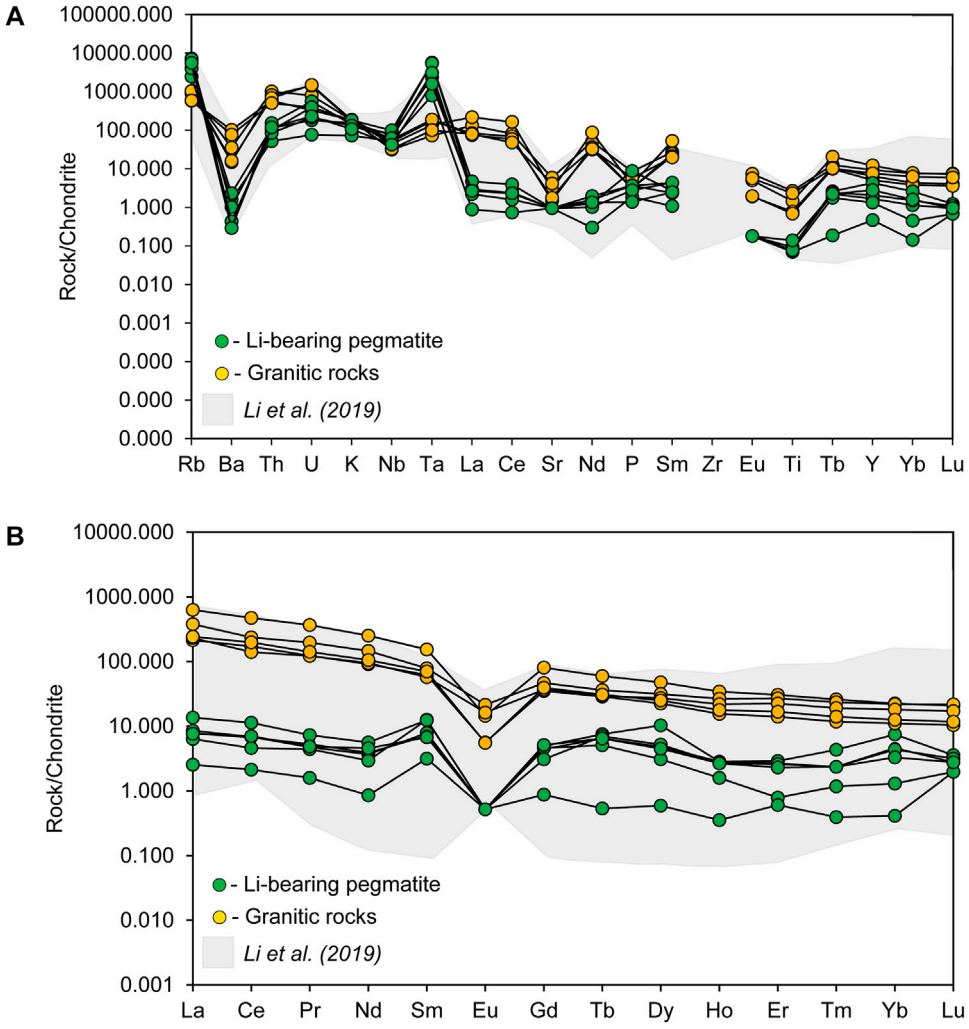

FIGURE 7
(A) Chondrite-normalized spider diagrams (chondrite values from Sun and McDonough, 1989) and **(B)** chondrite-normalized REE patterns (chondrite values from Sun and McDonough, 1989) of the Li-bearing pegmatites and related granitic rocks in the Phang Nga area, southern Thailand.

5 Discussion

5.1 Petrogenesis

The studied Li-bearing pegmatites and granites have porphyritic textures and significant amounts of biotite and muscovite, which are typical characteristics of the S-type granite in WBG (Nakapadungrat and Putthapiban, 1992; Charusiri et al., 1993). In addition, the presence of ilmenite in the rocks potentially indicates an ilmenite series (Ishihara, 1977), which is also consistent with the typical classified granites in the WBG (Cobbling et al., 1992; Nakapadungrat and Putthapiban, 1992; Putthapiban, 2002). The enrichment of LILEs (e.g., Rb and K) and the depletion of Ba, Nb, and Ti in the chondrite-normalized spider diagrams (Figure 7A) suggest collisional granite (Yao et al., 2014). The positive Rb and Th anomalies and low Yb together with LREE enrichment indicate that the rocks were derived from crustal sources (Yao et al., 2014). The chondrite-normalized REE patterns of both groups showing slightly high LREE patterns with negative Eu anomalies indicate fractional crystallization with plagioclase fractionation (Rollinson, 1993). The slightly positive Sm anomaly in the Li-bearing pegmatites might be related to the monazite crystallization caused by increasing fractionation (Cerny, 1991b). Moreover, the decreasing $(La/Yb)_N$ ratios and total REE concentrations (∑REE) from the granitic rocks to the Li-bearing pegmatites suggest the evolution of fractional-crystallization-related plagioclase (Yin et al., 2019). The depletion of Ti might have been caused by the fractional crystallization of Fe–Ti oxides (ilmenite) (Yin et al., 2019). The TAS plot (Figure 6) reflects that both the Li-bearing pegmatites and the granitic rocks have a subalkali composition, comparable with the composition plot of the WBG reported by Nakapadungrat and Putthapiban (1992) and Li et al. (2019).

The SiO_2 and Na_2O+K_2O–CaO plot (Figure 8A) of Frost et al. (2001) indicated that the Li-bearing pegmatites were of the alkalic to alkalic-calcic series, whereas the granites were of the

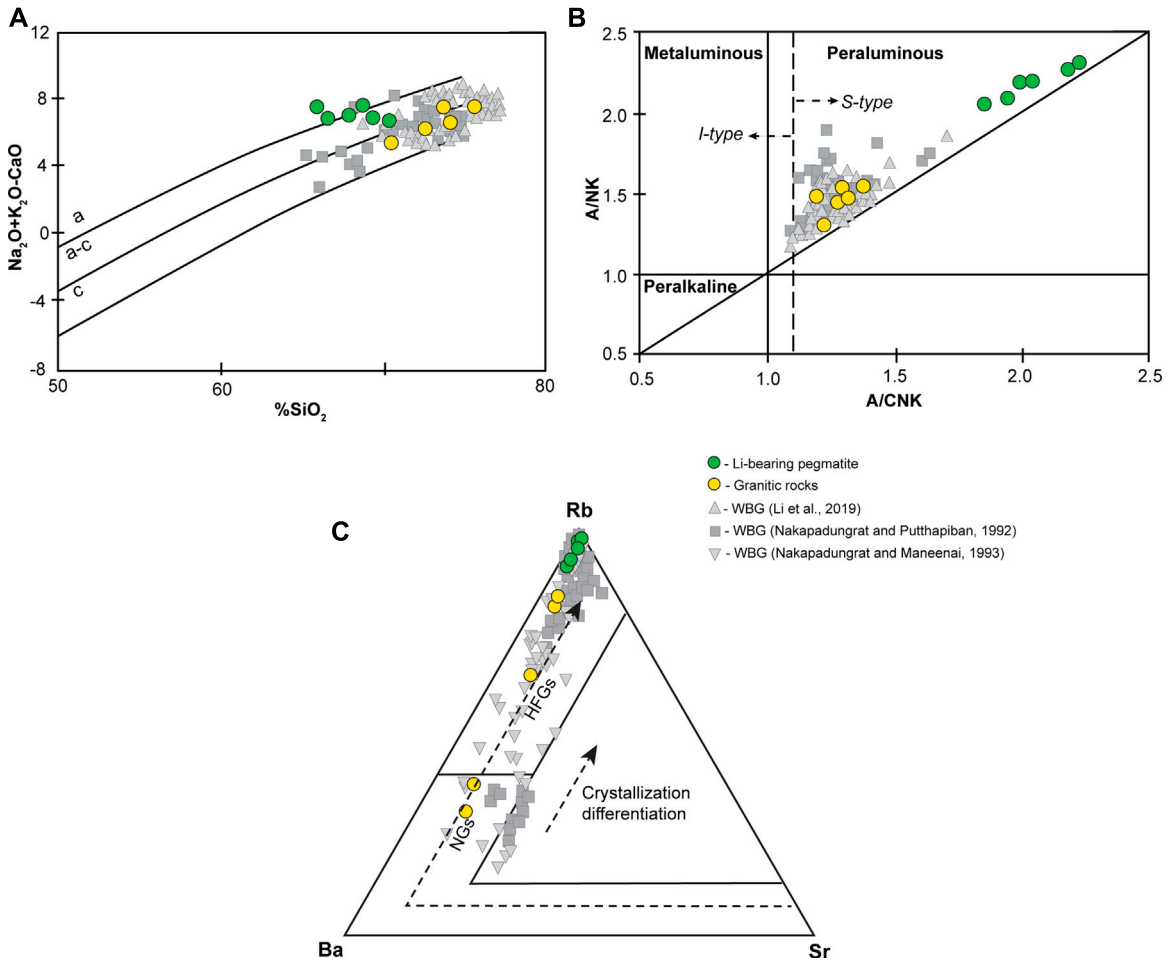

FIGURE 8
Plots of **(A)** SiO_2 and Na_2O+ K_2O–CaO diagram (after Frost et al., 2001); **(B)** Al/(Na + K) and Al/(Ca + Na + K) diagram (after Shand, 1943); **(C)** Ba–Rb–Sr ternary diagram (after Bouseily and Sokkary, 1975) of the Li-bearing pegmatites and related granitic rocks in the Phang Nga area, southern Thailand.

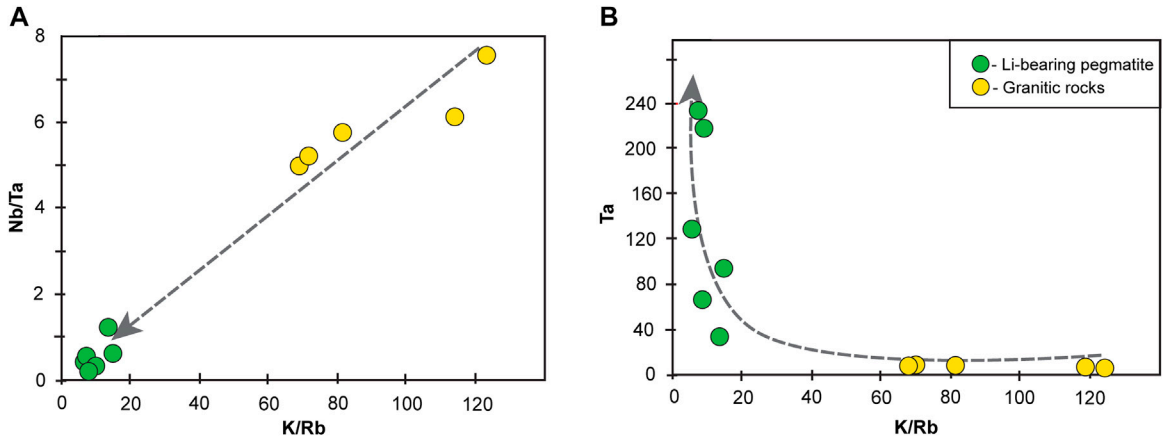

FIGURE 9
Plots of **(A)** K/Rb and Nb/Ta and **(B)** K/Rb and Ta diagrams (after Yin et al., 2019) of the Li-bearing pegmatite and related granitic rocks in the Phang Nga area, southern Thailand.

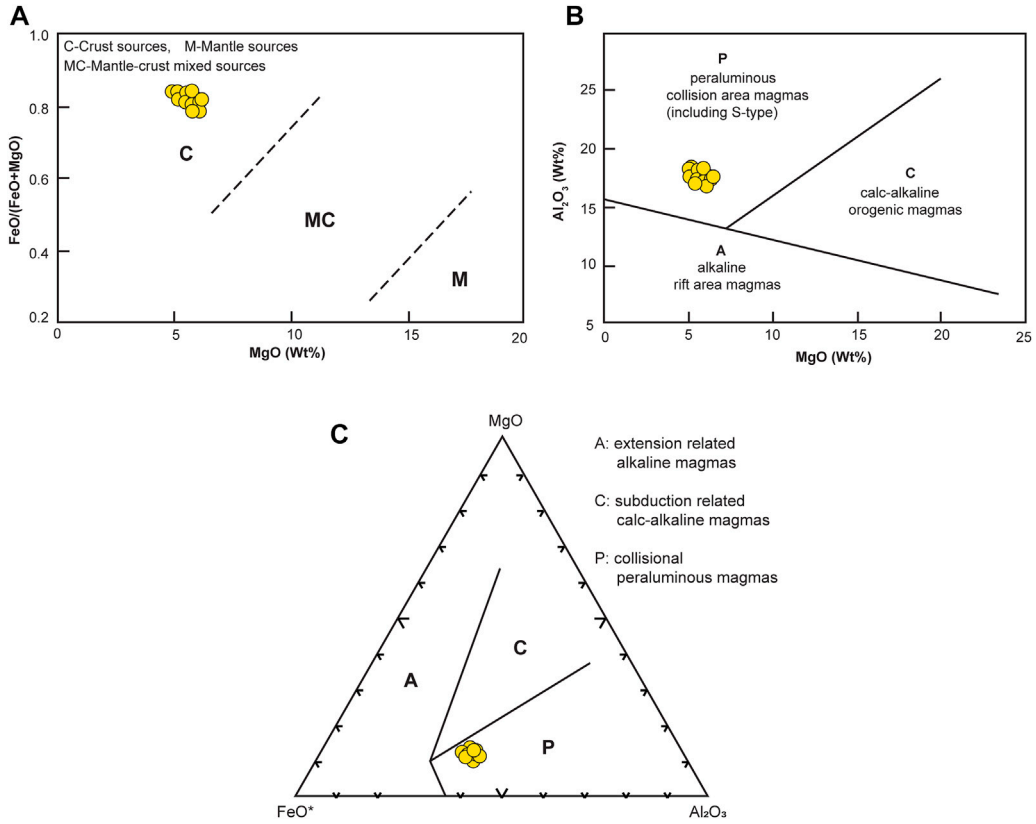

FIGURE 10
Biotite mineral chemistry plots of **(A)** MgO and MgO/(FeO + MgO) diagram (after Zhou, 1986), **(B)** MgO and Al_2O_3 diagram (after Abdel-Rahman, 1994), and **(C)** FeO*–MgO–Al_2O_3 diagram (after Abdel-Rahman, 1994).

calc-alkaline to alkalic-calcic series. In comparison, the plot of Al/(Ca + Na + K) against Al/(Na + K) of Shand (1943) clearly reflected that both the Li-bearing pegmatites and the granitic rocks were from peraluminous magma with S-type granite affinity (Figure 8B). Moreover, a plot of the Ba–Rb–Sr ternary diagram for the differentiation trend of granitic magma (Bouseily and Sokkary, 1975) (Figure 8C) shows a crystallization trend from the granitic rocks to the Li-bearing pegmatites, which potentially reflect the evolution of peraluminous granitic magma (Shen et al., 2022). Plots of Nb/Ta *versus* K/Rb (Yin et al., 2019) (Figure 9A) indicate the differentiation trend of granitic magma that links the granitic rocks to the Li-bearing pegmatites. Similarly, the plots of Ta *versus* K/Rb of Yin et al. (2019) (Figure 9B) also reflected the differentiation trend of the granitic magma of the granitic rocks to the Li-bearing pegmatites, respectively. These trends of high fractional crystallization are consistent with the crystallization features of the relationship of those highly evolved biotite granites to Li-mica granites in the Dahutang deposit, Southern China (Yin et al., 2019). The chemistry of mineral compositions seem to elucidate a relationship between the granitic rocks and the Li-bearing pegmatites in both K-feldspar and plagioclase. Moreover, the mineral chemistry of biotite (Figure 10) can reflect magmatic characteristics (Abdel-Rahman, 1994; Tukpho and Fanka, 2021; Zhao et al., 2022). The plot of Mg and FeO/(FeO + MgO) (Figure 10A) clearly indicates that the rocks were generated from crustal sources. In addition, the plots of MgO and Al_2O_3 (Figure 10B) and FeO–MgO–Al_2O_3 ternary diagram (Figure 10C) of Abdel-Rahman (1994) indicate collisional peraluminous magma related to S-type granite.

The crystallization pressure–temperature (P–T) conditions of the studied granitic rocks have been widely studied using mineral chemistry data of single minerals or coexisting minerals (e.g., Henry et al., 2005; Uchida et al., 2007; Fanka et al., 2018; Tukpho and Fanka, 2021). For instance, according to the biotite composition of the granitic rocks related to the Li-bearing pegmatites the mineral chemistry of biotite was used for calculating the crystallization P–T conditions of the rocks using the biotite geothermometer of Henry et al. (2005) and the biotite geobarometer of Uchida et al. (2007). Meanwhile, the Ti-in-biotite geothermometer of Henry et al. (2005) was used to calculate the crystallization temperature using the following equation: $T = \{[\ln(\mathrm{Ti}) - a - c\ (X_{\mathrm{Mg}})^3]/b\}^{0.333}$, where T is the temperature in degree Celsius, Ti is the number of atoms per formula unit on the basis of O = 22 atoms, X_{Mg} is Mg/(Mg + Fe), $a = -2.3594$, $b = 4.6482 \times 10^{-9}$, and $c = -1.7283$. The calculated crystallization temperatures of the granitic rocks related to the Li-bearing pegmatites ranged from 622°C to 675°C (with an average of 652°C) (Table 2). The calculated temperature in this study is probably comparable with the crystallization

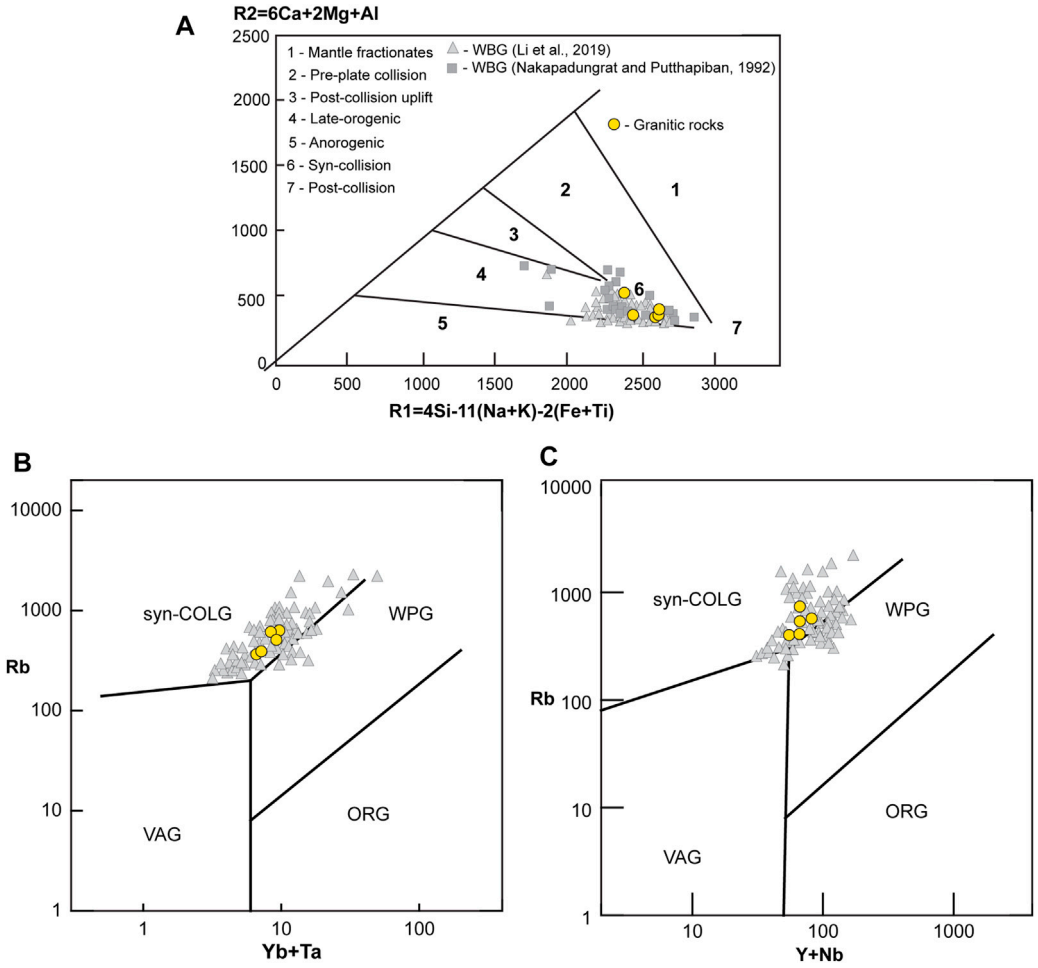

FIGURE 11
Plots of **(A)** R1 (4Si-11(Na + K)-2(Fe + Ti)) and R2 (6 Ca + 2 Mg + Al) tectonic discrimination diagrams (after Batchelor and Bowden, 1985); **(B)** Yb + Ta and Rb diagram (after Pearce et al., 1984); **(C)** Y + Nb and Rb diagram (after Pearce et al., 1984).

temperature of highly evolved peraluminous granitic melts (<650°C; London, 2008; Wu et al., 2020; Shen et al., 2022) and slightly lower than the crystallization temperature of normal S-type granite (795°C; Chappell and White, 1992). The plots of the differentiation trend of granitic magma (Bouseily and Sokkary, 1975) presented in Figure 8C together with the Nb/Ta and K/Rb (Figure 9A) and Ta vs. K/Rb (Figure 9B) plots for the relationship trends (Yin et al., 2019) reflect a highly differentiated granitic magma (Shen et al., 2022) that started from granitic rocks as the parental granite to the Li-bearing pegmatite, respectively. Therefore, the granitic rocks and the Li-bearing pegmatites were probably produced from the same parental granitic magma crystallized at a low crystallization temperature of about 652°C for the granitic rocks and at a lower temperature for the Li-bearing pegmatites, consistent with the differentiation of the granitic rocks to the Li-bearing pegmatites in the Koktolay deposits, China (Shen et al., 2022).

In terms of crystallization pressures, the Al-in-biotite geobarometer of Uchida et al. (2007) was applied to calculate the crystallization pressure using the following equation: P (kbar) = 3.03 × ^{T}Al–6.53 (±0.33), where ^{T}Al is the total content in biotite based on O = 22. The calculation pressures of the granitic rocks related to the Li-bearing pegmatites were 3.49–4.25 kbar, with an average of 3.87 kbar (Table 2). In addition, the calculated pressures were widely used to estimate the equilibration depth of plutonic rocks (e.g., Stein and Dietl, 2001; Helmy et al., 2004; Hossain et al., 2009; Fanka et al., 2016; 2018) using the following equation: $P = \rho gh$, where P represents pressure (Gpa), ρ is the continental crust density (2.73 km/m^3), g is the specific gravity (10.0 m/s^2), and h represents depth (km). The intrusion depths estimated from the crystallization pressures of this study are presented in Table 2. The emplacement depths ranged from 13 to 15 km (depth$_{av.}$ = 14 km), corresponding to the middle–upper crust level (Petrini and Podladchikov, 2000; Ramo, 2005; Fanka et al., 2018). Moreover, the emplacement depths were consistent with the calculated crystallization temperatures (622°C–675°C), which also indicate a middle–upper crust level (Peacock, 1993; Winter, 2001; Kelemen et al., 2003; Richards, 2003) with a geothermal gradient of about 20°C–40°C (Rothstein and Manning, 2003; Annen et al., 2006).

TABLE 7 Overview of the Li grade from Li-pegmatites in the main lithium deposits in the world.

Country	Deposits	Lithium grade (%Li)	Type of deposit	Reference
Thailand	(1) Thailand: Phang Nga	0.43	Lepidolite granite	This study
Vietnam	(2) Vietnam: La Vi, Quang Ngai	0.51	Lepidolite granite	Hien-Dinh et al. (2017)
China	(3) China: Jiajika	0.59	Spodumene pegmatite	Research In China (2009)
China	(4) China: Koktokay no.3	1.25	Spodumene-Lepidolite pegmatite	Chen et al. (2022)
China	(5) China: Bailongshan	0.7	Spodumene pegmatite	Wang et al. (2021)
China	(6) China: Qiongjiagan	0.6	Spodumene pegmatite	Qin et al. (2021)
China	(7) China: Jiangxi	0.77	Amblygonite pegmatite	Wang et al. (2020)
China	(8) China: South Fulugou	0.88	Spodumene pegmatite	Gao et al. (2020)
China	(9) China: Kalaka	0.43	Spodumene pegmatite	Teng and Gao (2019)
China	(10) China: Aktas	0.7	Spodumene pegmatite	Teng and Gao (2019)
Kazakhstan	(11) Kazakhstan: Kalba	0.95	Spodumene pegmatite	Oitseva et al. (2017)
America	(12) United States: Kings Mountain	0.70	Spodumene pegmatite	Kesler (1978)
America	(13) United States: Bessemer City	0.67	Spodumene pegmatite	Kesler (1978)
Canada	(14) Canada: Whabouchi	0.54	Spodumene pegmatite	Groves et al. (2022)
Canada	(15) Canada: Georgia Lake	0.53	Spodumene pegmatite	Breaks et al. (2008)
Canada	(16) Canada: Separation Rapids	0.61	Spodumene pegmatite	Sweetapple (2000)
Canada	(17) Canada: Tanco	0.64	Spodumene-Petalite pegmatite	Stilling et al. (2006)
Canada	(18) Canada: James Bay	0.58	Spodumene pegmatite	SRK Consulting (2010)
Canada	(19) Canada: Quebec Lithium	0.23	Spodumene pegmatite	Canada Lithium Corp. (2012)
Australia	(20) Australia: Greenbushes	1.05	Spodumene pegmatite	Groves et al. (2022)
Australia	(21) Australia: Mt. Cattlin	0.67	Spodumene pegmatite	(www.galaxyresources.com.au)
Australia	(22) Australia: Kathleen Valley	0.65	Spodumene pegmatite	Groves et al. (2022)
Australia	(23) Australia: Pilgangoora	0.58	Spodumene pegmatite	Groves et al. (2022)
Australia	(24) Australia: Mt. Marion	0.64	Spodumene pegmatite	Groves et al. (2022)
Zimbabwe	(25) Zimbabwe: Bikita	0.65	Spodumene-Petalite pegmatite	Bradley et al. (2017)
Zimbabwe	(26) Zimbabwe: Kamativi belt	0.28	Spodumene pegmatite	Sinclair (1996)
Congo	(27) Congo: Manono-Kitolo	0.6	Spodumene pegmatite	Sinclair (1996)
Mali	(28) Mali: Goulamina	0.69	Spodumene pegmatite	Groves et al. (2022)
Namibia	(29) Namibia: Rubicon and Helikon	1.4	Lepidolite-Petalite pegmatite	Kesler (1978)
Portugal	(30) Portugal: Fregeneda-Almendra	0.3	Spodumene-Lepidolite-Petalite pegmatite	EDICOES (1998)
Finland	(31) Finland: Ullava Länttä	0.43	Spodumene pegmatite	Keliber Nordic Mining (2012)
Russia	(32) Russia: Kolmozero	0.53	Spodumene pegmatite	Groves et al. (2022)
Russia	(33) Russia: Vishnyakovskoe	0.49	Spodumene-Petalite pegmatite	Seltmann et al. (2010); Zagorsky et al. (2014)
Russia	(34) Russia: Goltzovoe	0.37	Spodumene-Petalite pegmatite	Seltmann et al. (2010); Vladimirov et al. (2012)
Russia	(35) Russia: Zavitinskoye	0.37	Spodumene pegmatite	Seltmann et al. (2010); Melentiev et al. (2022)
Russia	(36) Russia: Alakha	0.46	Lepidolite pegmatite	Annikova et al., (2016)
Russia	(37) Russia: Tastyq	1.86	Spodumene pegmatite	Kuznetsova and Prokof'ev, (2009)

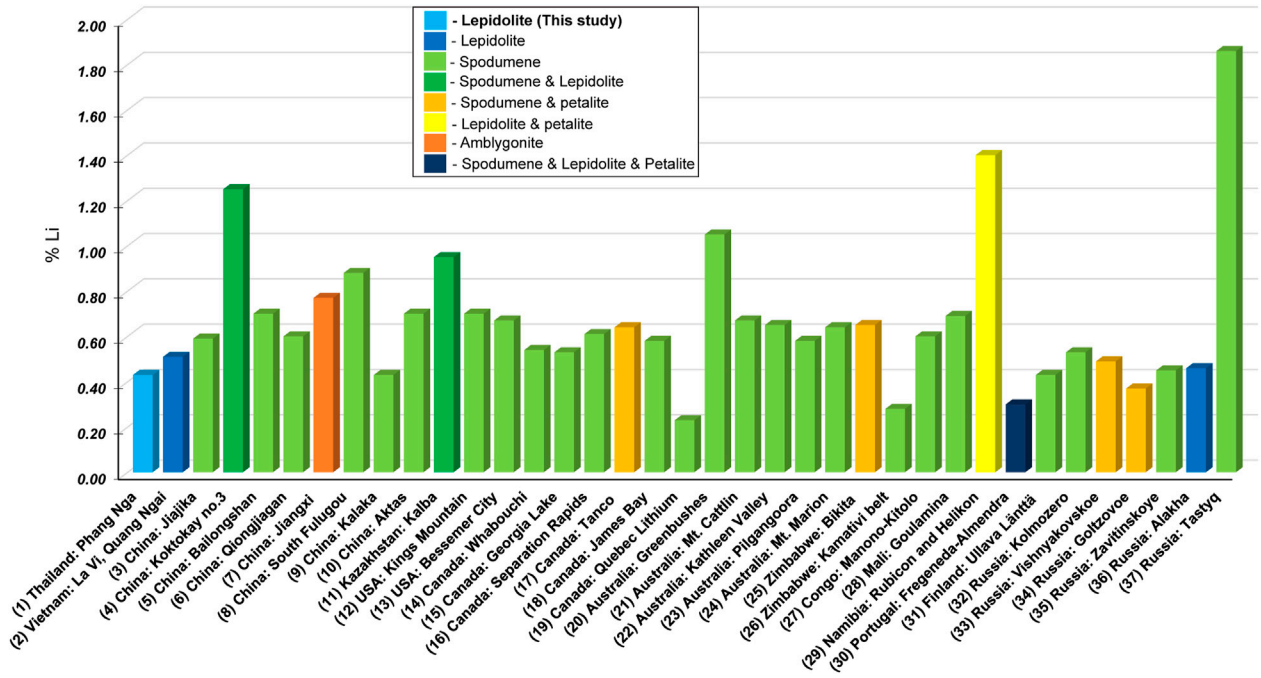

FIGURE 12
Overview of the Li grade of the Li-bearing pegmatites in the Phang Nga area, southern Thailand, and lithium deposits in the world. The details of the Li grades of the lithium deposits are presented in Table 7.

5.2 Tectonic implications

The tectonic setting of the study area (Phang Nga, southern Thailand) in the WBG as part of the SE Asia tin belt is implied by the combination of mineral chemistry and whole-rock geochemistry together with the findings of previous studies on the WBG. The geochemical plot of R1 (4Si-11(Na + K)-2(Fe + Ti)) and R2 (6Ca + 2 Mg + Al) diagrams (Figure 11A) suggest that the granitic rocks and the Li-bearing pegmatites relate to a syn-collision setting comparable with that of the WBG in Thailand reported by Nakapadungrat and Putthapiban (1992) and the WBG in Myanmar (Li et al., 2019). Moreover, the plots of the Yb + Ta *versus* Rb diagram (Figure 11B) and the plot of the Y + Nb and Rb diagram (Figure 11C) clearly indicate that these rocks are emplaced in syncollision granite. These diagrams are clearly consistent with the reported WBG in Myanmar (Li et al., 2019). Moreover, the mineral chemistry of biotite plotted in the MgO *versus* Al_2O_3 (Figure 10B) and FeOt–MgO–Al_2O_3 ternary (Figure 10C) diagrams also indicate a peraluminous magma related to a collision setting.

The LILE enrichment (including Rb, Ta, and K) in the chondrite-normalized spider diagram (Figure 7A) and the depletion of Ba, Nb, Ti, and Yb indicate an S-type-granite–related collision (Grosse et al., 2011). This collision is strongly supported by the magmatic event related to granitic rocks during the collision of the West Burma and Sibumasu terranes during the Cretaceous to Eocene (Nakapadungrat and Putthapiban, 1992; Charusiri et al., 1993; Watkinson et al., 2011; Li et al., 2019). The geochronology of granitic rocks reported in the Phang Nga area (e.g., Garson et al., 1975; Nakapadungrat et al., 1985; Chrusiri, 1989) includes Khao Lak (78 Ma; Nakapadungrat et al., 1985), Khao Khanim (65 Ma; Garson et al., 1975), Khao Kata Khwam (72 Ma; Charusiri, 1989), and Khao Po (52 Ma; Garson et al., 1975) and other areas along the WBG (Nakapadungrat and Putthapiban, 1992; Charusiri et al., 1993; Li et al., 2019).

Geochronological reports indicate collisional events during the Late Cretaceous and Paleocene to the Eocene (Nakapadungrat and Putthapiban, 1992; Charusiri et al., 1993; Li et al., 2019) related to S-type granite and related mineralization (Nakapadungrat and Maneenai, 1993; Li et al., 2019). The Late Cretaceous (88–65 Ma) (Nakapadungrat and Putthapiban, 1992; Charusiri et al., 1993; Li et al., 2019) probably reflect peraluminous S-type granites in the Khao Lak, Khao Kata Khwam, and Khao Khanim areas (Figure 1B) and related Sn–W mineralization (e.g., Nok Hook Sn mine in Khao Kata Khwam area; Figure 1B) (Nakapadungrat and Maneenai, 1993) of the WBG. Moreover, Paleocene to Eocene (60–50 Ma) magmatism (Garson et al., 1975; Charusiri et al., 1993) is also reported for the emplacement of granitic rocks in the WBG and the study area (e.g., the Khao Po area; Figure 1B) and related Sn–W mineralized pegmatites (Nakapadungrat and Maneenai, 1993), including the Li-bearing pegmatites of this study reflected by a cassiterite assemblage (Figure 5).

5.3 Lithium deposit and potential

The combined field occurrence, petrography, mineral chemistry, and geochemistry data indicate that the granitic rocks and related Li-bearing pegmatites in the Phang Nga,

southern Thailand, have a close relationship, as reflected by the highly fractional crystallization trend in the plots of Ba–Rb–Sr (Figure 8C), Nb/Ta vs. K/Rb (Figure 9A), and Ta vs. K/Rb (Figure 9B). This probably indicates that the Li-bearing pegmatites are part of the late stages of the highly fractionated granitic magma in the study area (Yin et al., 2019). The close relationship of the Li-bearing pegmatites and highly fractionated granitic rocks, such as tourmaline–muscovite granite, was also mentioned in a study on the Nok Hook mine, Khao Kata Khwam area (Figure 1B) (Suwimonprecha, 1989; Nakapadungrat and Maneenai, 1993). This relationship is strongly consistent with those of highly fractionated granites and Li-bearing pegmatites in several areas, such as the Dahutang deposit, South China (Yin et al., 2019), Separation Lake area, Ontario, Canada (Tindle and Breaks, 2000), Gonçalo, central Portugal (Neiva and Ramos, 2010), and Maine, United States (Marchal et al., 2014), which can be linked link to the cogenetic granite and Li-pegmatite formation model (Cerny, 1991) from Li-barren granite to REE-Be–bearing pegmatite, REE-Be-Nb-Ta–bearing pegmatite, and Li-Cs-Be-Nb-Ta–bearing pegmatite (Cerny, 1991; Muller et al., 2022). Moreover, pegmatite formation related to granite according to Cerny (1991a), Cerny (1991b) for pegmatite migration from the rare-metal-barren granitic rocks to rare-metal-bearing pegmatite (Li, Cs, Sn, Nb, Ta enrichment) is consistent with the reported pegmatites in the Phang Nga–Phuket area, southern Thailand, classified into Sn–Ta–Nb–mica free pegmatite and Sn–Li–F–W–Ta–Nb–REE–mica–rich pegmatite (Gocht and Pluhar, 1982). The Li-bearing pegmatites exposed in the study area (Figure 1B) are well-defined as Sn–W mineralized granites in the SE Asia tin belt (Cobbing et al., 1986; Nakapadungrat and Putthapiban, 1992; Nakapadungrat and Maneenai, 1993). The Sn–W deposits related to these granitic rocks are mainly discovered in endogenous quartz–cassiterite–wolframite vein swarms, argillic disseminations, and lepidolite pegmatite types (Nakapadungrat and Maneenai, 1993). In this study, lepidolite pegmatite, one of the Sn–W sources in Thailand, is defined as the Li-bearing pegmatites in the Khao Po area (Figure 1B), considered as one of the large unzoned lepidolite pegmatites in the world (Garson et al., 1975).

For the Li grade, the Li content of the Li-bearing pegmatites was 0.43% Li (0.17%–0.65% Li) in this study, comparable with those of other Li-bearing pegmatites in the world (Table 7; Figure 12). According to the overall Li deposits in the world (Table 7; Figure 12), high Li grades are found in spodumene pegmatite deposits, such as the Tastyq deposits in Russia (1.86% Li; Kuznetsova and Prokof'ev, 2009), the Greenbushes deposits in Australia (1.05% Li; Groves et al., 2022), the Kalba deposits in Kazakhstan (0.95% Li; Oitseva et al., 2017; Khromykh et al., 2020; D'yachkov et al., 2021; Zimanovskaya et al., 2022) and the South Fulugou deposits in China (0.88% Li; Gao et al., 2020). These are followed by spodumene, lepidolite, and petalite pegmatite deposits, such as the Rubicon and Helikon deposits in Namibia (1.40% Li; Kesler, 1978) and the Koktokay no. 3 deposits in China (1.25% Li; Wang et al., 2021). In addition, amblygonite pegmatite deposits are also high-Li-grade sources, as reported in the Jiangxi deposits in China (0.77% Li; Wang et al., 2020). For the Li-bearing pegmatites in this study, the Li grade is probably the same as those of the well-known lepidolite pegmatite deposits in the world, such as those in La Vi, Quang Ngai, Vietnam (0.51% Li; Hien-Dinh et al., 2017), Zavitinskoye, Russia (0.37% Li; Seltmann et al., 2010; Melentiev et al., 2022), and Alakha, Russia (0.46% Li; Annikova et al., 2016) (Table 7; Figure 12). Moreover, the Li grade in the lepidolite type of this study is also slightly higher than those of some well-known spodumene pegmatite deposits, such as the Kalaka deposit in China (0.43% Li; Teng and Gao, 2019), the Quebec Lithium in Canada (0.28% Li; Canada Lithium Corp., 2012), and the Kamativi belt in Zimbabwe (0.23% Li; Sinclair, 1996). For the Li grade in spodumene and petalite pegmatite deposits, some deposits have lower grades than that in this study, such as the Fregeneda–Almendra deposit in Portugal (0.3% Li; EDICOES, 1998) and the Goltzovoe deposit in Russia (0.37% Li; Seltmann et al., 2010; Vladimirov et al., 2012) (Table 7; Figure 12).

6 Conclusion

The Li-bearing pegmatites and related granitic rocks in the Phang Nga area, southern Thailand, can elucidate geological processes for petrogenesis, tectonic implications, and Li-mineralization together with the Li potential in Thailand as follows.

1. The Li-bearing pegmatites are characterized by lepidolite pegmatite and relate to the granitic rocks including porphyritic biotite–muscovite granite, biotite granite, and muscovite–tourmaline granite.
2. The geochemical characteristics of both the Li-bearing pegmatites and related granitic rocks indicate a peraluminous S-type granite affinity.
3. The enrichment of LILEs (e.g., Rb and K) and the depletion of Ba, Nb, and Ti together with the slightly high LREE contents indicate that the studied rocks were emplaced from a collisional setting.
4. The Li-bearing pegmatites that evolved from highly fractionated S-type granitic rocks are comparable with the WBG in Thailand, which took place during the West Burma and Sibumasu collision during the Cretaceous to Eocene.
5. The crystallization P–T conditions of the granitic rocks related to Li-bearing pegmatites were 3.49–4.25 kbar and 622°C–675°C, respectively, with an emplacement depth of 13–15 km.
6. The Li-bearing pegmatites, being among the Sn–W pegmatite deposits in southern Thailand, SE Asia tin belt, evolved from granitic rocks.
7. The Li-bearing pegmatites contained an average Li grade of 0.43% Li (0.17%–0.65% Li), which is similar to those of several well-known Li-bearing pegmatites in the world.

Data availability statement

The original contributions presented in the study are included in the article/supplementary material, further inquiries can be directed to the corresponding author.

Author contributions

AF contributed to the research initiation, field investigation, sample collection, laboratory studies, data collection, discussion, manuscript preparation, and revision. JT contributed to the laboratory studies and data collection. All authors contributed to the article and approved the submitted version.

Funding

This research was funded by the Thailand Science Research and Innovation Fund Chulalongkorn University [CU_FFB65_ind (3) _108_23_38].

Acknowledgments

The authors would like to acknowledge the Department of Geology, Faculty of Science, Chulalongkorn University, for the laboratory studies, the Pan Asia Metal (Thailand) Company Limited, and Mr. Sakda Thorraneethip for the support regarding the samples and accessible study site. The authors would like to thank the Department of Primary Industries and Mines and Miss Alissara Prasertying for the valuable discussions.

Conflict of interest

The authors declare that the research was conducted in the absence of any commercial or financial relationships that could be construed as a potential conflict of interest.

Publisher's note

All claims expressed in this article are solely those of the authors and do not necessarily represent those of their affiliated organizations, or those of the publisher, the editors and the reviewers. Any product that may be evaluated in this article, or claim that may be made by its manufacturer, is not guaranteed or endorsed by the publisher.

References

Abdel-Rahman, A. M. (1994). Nature of biotites from alkaline, calc-alkaline, and peraluminous magmas. *J. Pet.* 35, 525–541. doi:10.1093/petrology/35.2.525

Annen, C., Blundy, J. D., and Sparks, R. S. J. (2006). The Genesis of intermediate and silicic magmas in deep crustal hot zones. *J. Pet.* 47, 505–539. doi:10.1093/petrology/egi084

Annikova, I. Y., Vladimirov, A. G., Smirnov, S. Z., and Gavryushkina, O. A. (2016). Geology and mineralogy of the Alakha spodumene granite porphyry deposit, gorny altai, Russia. *Geol. Rudn. Mest.* 58, 404–426. doi:10.1134/s1075701516050020

Averill, W. A., and Olson, D. L. (1978). A review of extractive processes for lithium from ores and brines. *Energy* 3, 305–313. doi:10.1016/0360-5442(78)90027-0

Batchelor, R. A., and Bowden, P. (1985). Petrogenetic interpretation of granitoid rock series using multicationic parameters. *Chem. Geol.* 48, 43–55. doi:10.1016/0009-2541(85)90034-8

Bouseily, A. M., and Sokkary, A. A. (1975). The relation between Rb, Ba and Sr in granitic rocks. *Econ. Geol.* 16, 207–219. doi:10.1016/0009-2541(75)90029-7

Bradley, D. C., McCauley, A. D., and Stillings, L. L. (2017). *Mineral-deposit model for lithium- cesium-tantalum pegmatites*. Reston: U.S. Geological Survey.

Breaks, F. W., Selway, J. B., and Tindle, A. G., 2008. The Georgia Lake rare-element pegmatite field and related S-type, peraluminous granites, Quetico Subprovince, north-central Ontario: Ontario Geological Survey, Open File Report 6199.

Canada Lithium Corp (2012). Lithium: Driving our growth. Available at: http://www.canadalithium.com/s/QuebecLithium.asp.

Cerny, P. (1991b). Rare-element granitic pegmatites, Part II. Regional to global environments and petrogenesis. *Geosci. Can.* 18, 68–81.

Cerny, P. (1991a). Rare-element granitic pegmatites. Part I: Anatomy and internal evolution of pegmatite deposits. *Geosci. Can.* 18, 49–67.

Chappell, B. W., and White, A. J. R. (1992). I- and S-type granites in the lachlan fold belt. *Earth Env. Sci. Trans. R. So.* 83, 1–26. doi:10.1017/s0263593300007720

Charusiri, P., Clark, A. H., Farrar, E., Archibald, D., and Charusiri, B. (1993). Granite belts in Thailand: Evidence from the $^{40}Ar/^{39}Ar$ geochronological and geological synthesis. *J. Southeast Asian Earth Sci.* 8, 127–136. doi:10.1016/0743-9547(93)90014-g

Charusiri, P., Daorerk, V., Archibald, D., Hisada, K., and Am-paiwan, T. (2002). Geotectonic evolution of Thailand, a new synthesis. *J. Geol. Soc. Thail.* 1, 1–20.

Charusiri, P. (1989). "Lithophile metallogenetic epochs of Thailand: A geological and geochronological investigation," (Ontario, Canada: Queen's University), 819. Unpublished PhD thesis.

Chen, J., Zhang, H., Tang, Y., Lv, Z., An, Y., Wang, M., et al. (2022). Lithium mineralization during evolution of a magmatic–hydrothermal system: Mineralogical evidence from Li-mineralized pegmatites in Altai, NW China. *Ore Geol. Rev.* 149, 105058. doi:10.1016/j.oregeorev.2022.105058

Cobbing, E. J., Mallick, D. I. J., Pitfield, P. E. J., and Teoh, L. H. (1986). The granites of the Southeast asian tin belt. *J. J. Geol. Soc. Lond.* 143, 537–550. doi:10.1144/gsjgs.143.3.0537

Cobbing, E. J., Pitfield, P., Darbyshire, D., and Mallick, D. (1992). *The granites of the Southeast asian tin belt*. London: Overseas Memoirs of the British Geological Survey.

Cox, K. G., Bell, B. G., and Pankhurst, R. J. (1979). *The interpretation of igneous rocks*. London: Unwin Hyman, 450.

Deer, W. A., Howie, R. A., and Zussman, J. (1966). *An introduction to the rock-forming minerals*. London: Longmans, 528.

Deer, W. A., Howie, R. A., and Zussman, J. (2013). *An introduction to the rock-forming minerals* 3rd ed. London: Longmans, 549.

DMR (1985). *Geological map of Thailand scale 1:250,000 sheet NC47-14 changwat phangnga*.

DMR (2009). *Standard of characteristics of tin deposits and application*. Bangkok, Thailand: Department of Mineral Resources, 60.

D'yachkov, B. A., Bissatova, A. Y., Mizernaya, M. A., Khromykh, S. V., Oitseva, T. A., Kuzmina, O. N., et al. (2021). Mineralogical tracers of gold and rare-metal mineralization in eastern Kazakhstan. *Minerals* 11, 253. doi:10.3390/min11030253

EDICOES (1998). Mineral potential of Portugal other metals. Available at: http://e-geo.ineti.pt/edicoes_online/diversos/potential/capitulo6.htm.

Fanka, A., Tsunogae, T., Daorerk, V., Tsutsumi, Y., Takamura, Y., Endo, T., et al. (2016). Petrochemistry and mineral chemistry of late permian hornblendite and hornblende gabbro from the Wang nam khiao area, nakhon ratchasima, Thailand: Indication of palaeo-tethyan subduction. *J. Asian Earth Sci.* 130, 239–255. doi:10.1016/j.jseaes.2016.11.018

Fanka, A., Tsunogae, T., Daorerk, V., Tsutsumi, Y., Takamura, Y., and Sutthirat, C. (2018). Petrochemistry and zircon U-Pb geochronology of granitic rocks in the Wang Nam Khiao area, Nakhon Ratchasima, Thailand: Implications for petrogenesis and tectonic setting. *J. Asian Earth Sci.* 157, 92–118. doi:10.1016/j.jseaes.2017.08.025

Frost, B. R., Barnes, C. G., Collins, W. J., Arculus, R. J., Ellis, D. J., and Frost, C. D. (2001). A geochemical classification for granitic rocks. *J. Pet.* 42, 2033–2048. doi:10.1093/petrology/42.11.2033

Gao, Y., Bagas, L., Li, K., Jin, K., Liu, Y., and Teng, J. (2020). Newly discovered triassic lithium deposits in the dahongliutan area, north west China: A case study for the detection of lithium-bearing pegmatite deposits in rugged terrains using remote-sensing data and images. *Front. Earth Sci.* 8, 591966. doi:10.3389/feart.2020.591966

Garson, M. S., Young, B., Mitchell, A. H. G., and Tait, B. A. R. (1975). The geology of tin belt in peninsular Thailand around Phuket, Phangnga and Takua Pa. *Overseas Mem. Inst. Geol. Sci. lond.* 1, 112.

Gocht, W., and Pluhar, E. (1982). "Types of Phuket pegmatites with special reference to Ta-rich ores A," in *Mineralization associated with acid magmatism*. Editor M. Evan (United States: Wiley), 91–99.

Grosse, P., Bellos, L. I., de los Hoyos, C. R., Larrovere, M. A., Rossi, J. N., and Toselli, A. J. (2011). Across-Arc variation of the famatinian magmatic arc (NW Argentina) exemplified by I-S- and transitional I/S-type early ordovician granitoids of the sierra de Velasco. *J. Southeast Asian Earth Sci.* 32, 110–126. doi:10.1016/j.jsames.2011.03.014

Groves, D. I., Zhang, L., Groves, I. M., and Sener, A. K. (2022). Spodumene: The key lithium mineral in giant lithium-cesium-tantalum pegmatites. *Acta Pet. Sin.* 38, 1–8. doi:10.18654/1000-0569/2022.01.01

Helmy, H. M., Ahmed, A. F., El Mahallawi, M. M., and Ali, S. M. (2004). Pressure, temperature and oxygen fugacity conditions of calc-alkaline granitoids, Eastern Desert of Egypt, and tectonic implications. *J. Afr. Earth Sc.* 38, 255–268. doi:10.1016/j.jafrearsci.2004.01.002

Henry, D., Guidotti, C., and Thomson, J. (2005). The Ti-saturation surface for low-to-medium pressure metapelitic biotites: Implications for geothermometry and Ti-substitution mechanism. *Amer. Min.* 90, 31–328. doi:10.2138/am.2005.1498

Hien-Dinh, T. T., Dao, D. A., Tran, T., Wahl, M., Stein, E., and Giere, R. (2017). Lithium-rich albite-topaz-lepidolite granite from central Vietnam: A mineralogical and geochemical characterization. *Eur. J. Mineral.* 29, 35–52. doi:10.1127/ejm/2017/0029-2581

Hossain, I., Tsunogae, T., and Rajesh, H. M. (2009). Geothermobarometry and fluid inclusions of dioritic rocks in Bangladesh: Implications for emplacement depth and exhumation rate. *J. Asian Earth Sci.* 34, 731–739. doi:10.1016/j.jseaes.2008.10.010

Ishihara, S. (1977). The magnetite-series and ilmenite-series granitic rocks. *Min. Geol.* 27, 293–305.

Kelemen, P. B., Rilling, J. L., Parmentier, E. M., Mehl, L., and Hacker, B. R. (2003). Thermal structure due to solid-state flow in the mantle wedge beneath arcs. Inside the Subduction Factory. *AGU Monogr.* 138, 293–311.

Keliber Nordic Mining (2012). Spodumene deposits and lithium province. Available at: http://www.keliber.no/deposits/category229.html.

Kesler, T. L. (1978). Raw lithium supplies. *Min. Eng.* 1978, 283–285.

Khromykh, S. V., Oitseva, T. A., Kotler, P. D., D'yachkov, B. A., Smirnov, S. Z., Travin, A. V., et al. (2020). Rare-metal pegmatite deposits of the Kalba region, eastern Kazakhstan: Age, composition and petrogenetic implications. *Minerals* 10, 1017. doi:10.3390/min10111017

Kuznetsova, L. G., and Prokof'ev, Yu. (2009). Petrogenesis of extremely lithium-rich spodumene aplites of the Tastyg deposit, Sangilen highland, Tyva Republic. *Dokl. Earth Sci.* 429, 1262–1266. doi:10.1134/s1028334x09080054

Li, J.-X., Fan, W.-M., Zhang, L.-Y., Evans, N. J., Sun, Y.-L., Ding, L., et al. (2019). Geochronology, geochemistry, and Sr–Nd–Hf isotopic compositions of Late Cretaceous–Eocene granites in southern Myanmar: Petrogenetic, tectonic, and metallogenic implications. *Ore Geol. Rev.* 112, 103031. doi:10.1016/j.oregeorev.2019.103031

London, D. (2008). *Pegmatites*. Can. Mineral. Spec. Publ.

Marchal, K. L., Simmons, W. B., Falster, A. U., Webber, K. L., and Roda-Robles, E. (2014). Geochemistry, mineralogy, and evolution of Li-Al micas and feldspars from the mount mica pegmatite, Maine, USA. *Can. Mineral.* 52, 221–233. doi:10.3749/canmin.52.2.221

Melentiev, G. B., Yurgenson, G. A., and Delitzyn, L. M. (2022). Prospects and priorities for the reconstruction and development of lithium mining production on the basis of domestic raw materials. *IOP Conf. Ser. Earth Environ. Sci.* 962, 012055. doi:10.1088/1755-1315/962/1/012055

Morimoto, N., Fabries, J., Ferguson, A. K., Ginzburg, I. V., Ross, M., Seifert, F. A., et al. (1988). Nomenclature of pyroxene. *Am. Min.* 73, 1123–1133.

Muller, A., Reimer, W., Wall, F., Williamson, B., Menuge, J., Brönner, M., et al. (2022). Greenpeg – exploration for pegmatite minerals to feed the energy transition: First steps towards the green stone age. *Geol. Soc. Spec. Publ.* 526. doi:10.1144/sp526-2021-189

Nakapadungrat, S., and Putthapiban, P. (1992). "Granites and associated mineralization in Thailand," in *Proceedings of national conference on geologic resources of Thailand: Potential for future development*. Editor C. Piancharoen (Bangkok, Thailand: Department of Mineral Resources), 153–171.

Nakapadungrat, S., Beckinsale, R. D., and Suensilpong, S. (1985). "Geochronology and geology of Thai granites," in *Proc. Conf. Applications of Geology and the national development*. Editors N. Thiramongkol, S. Nakapadungrat, and V. Pisutha-Arnond (Bangkok, Thailand: Chulalongkorn University), 75–93.

Nakapadungrat, S., and Maneenai, D. (1993). The phuket, phangnga and Takua Pa tin-field, Thailand. *J. Southeast Asian Earth Sci.* 8, 359–368. doi:10.1016/0743-9547(93)90037-p

Neiva, A. M. R., and Ramos, J. M. F. (2010). Geochemistry of granitic aplite-pegmatite sillsand petrogenetic links with granites, Guarda-Belmonte area, central Portugal. *Eur. J. Mineral.* 22, 837–854. doi:10.1127/0935-1221/2010/0022-2072

Oitseva, T. A., Dyachko, B. A., Vladimirov, A. G., Kuzmina, O. N., and Ageeva, O. V. (2017). New data on the substantial composition of Kalba rare metal deposits. *IOP Conf. Ser. Earth Environ. Sci.* 110, 012018. doi:10.1088/1755-1315/110/1/012018

Peacock, S. M. (1993). Large-scale hydration of the lithosphere above subducting slabs. *Chem. Geol.* 108, 49–59. doi:10.1016/0009-2541(93)90317-c

Pearce, J. A., Harris, N. B. W., and Tindle, A. G. (1984). Trace element discrimination diagrams for the tectonic interpretation of granitic rocks. *J. Pet.* 25, 956–983. doi:10.1093/petrology/25.4.956

Petrini, K., and Podladchikov, Y. (2000). Lithospheric pressure-depth relationship in compressive regions of thickened crust. *J. Metamorph. Geol.* 18, 67–77. doi:10.1046/j.1525-1314.2000.00240.x

Putthapiban, P. (2002). "Geology and geochronology of the igneous rocks of Thailand," in *The symposium on Geology of Thailand* (Thailand: Bangkok), 261–283.

Qin, K. Z., Zhao, J. X., He, C. T., and Shi, R. Z. (2021). Discovery of the Qongjiagang giant lithium pegmatite deposit in Himalaya, Tibet, China. *Acta Pet. Sin.* 37, 3277–3286. in Chinese with English abstract. doi:10.18654/1000-0569/2021.11.02

Ramo, O. T. (2005). Granitic systems–a special issue in honor of Ilmari Haapala. *Lithos* 80. xi–xix. doi:10.1016/j.lithos.2004.09.015

Research in China (2009). China lithium carbonate industry report, Available at: http://www.researchinchina.com/FreeReport/PdfFile/633985558995235000.pdf.

Richards, J. P. (2003). Tectono-magmatic precursors for porphyry Cu-(Mo-Au) deposit formation. *Econ. Geol.* 98, 1515–1533. doi:10.2113/gsecongeo.98.8.1515

Rollinson, H. R. (1993). *Using geochemical data: Evaluation, presentation and interpretation*. Harlow, UK: Longman Scientific and Technical Ltd., 352.

Rothstein, D. A., and Manning, C. E. (2003). Geothermal gradients in continental magmatic arcs: Constraints from the eastern Peninsular Ranges batholith, Baja California. *México. Geol. Soc. Am. Spec. Pap.* 374, 337–354.

Seltmann, R., Soloviev, S., ShatovPirajno, F., Naumov, E., and Cherkasov, S. (2010). Metallogeny of siberia: Tectonic, geologic and metallogenic settings of selected significant deposits*. *Aust. J. Earth Sci.* 57, 655–706. doi:10.1080/08120099.2010.505277

Shand, S. J. (1943). *Eruptive rocks. Their genesis, composition, classification, and their relation to ore-deposits with a chapter on meteorite*. New York: John Wiley & Sons.

Shen, P., Pan, H., Li, C., Feng, H., He, L., Bai, Y., et al. (2022). Newly-recognized Triassic highly fractionated leucogranite in the Koktokay deposit (Altai, China): Rare-metal fertility and connection with the No. 3 pegmatite. *Gondwana Res.* 112, 24–51. doi:10.1016/j.gr.2022.09.007

Sinclair, W. D. (1996). "Granitic pegmatites," in *Geology of Canadian mineral deposit types: Geological survey of Canada, Geology of Canada*. Editors O. R. Eckstrand, W. D. Sinclair, and R. I. Thorpe (Ottawa: Canada Communication Group), 503–512.

Smith, J. V., and Brown, W. L. (1974). *Feldspar minerals*. Germany: Springer-Verlag, 1–690.

Sone, M., Metcalfe, I., and Chaodumrong, P. (2012). The chanthaburi terrane of southeastern Thailand: Stratigraphic confirmation as a disrupted segment of the sukhothai arc. *J. Asian Earth Sci.* 61, 16–32. doi:10.1016/j.jseaes.2012.08.021

Sone, M., and Metcalfe, I. (2008). Parallel tethyan sutures in mainland Southeast Asia: New insights for palaeo-tethys closure and implications for the indosinian orogeny. *Tectonics* 340, 166–179. doi:10.1016/j.crte.2007.09.008

SRK Consulting (2010). *Mineral resource evaluation, james bay lithium project, james bay, Quebec, Canada*. South Africa: SRK Consulting.

Stein, E., and Dietl, C. (2001). Hornblende thermobarometry of granitoids from the Central Odenwald (Germany) and their implications for the geotectonic development of the Odenwald. *Mineral. Pet.* 72, 185–207. doi:10.1007/s007100170033

Stilling, A., Cerny, P., and Vanstone, P. J. (2006). The Tanco pegmatite at Bernic Lake, Manitoba. XVI. Zonal and bulk compositions and the petrogenetic significance. *Can. Mineral.* 44, 599–623. doi:10.2113/gscanmin.44.3.599

Sun, S. S., and McDonough, W. F. (1989). Chemical and isotopic systematics of oceanic basalts: Implications for mantle composition and processes. *J. Geol. Soc. Lond.* 42, 313–345. doi:10.1144/gsl.sp.1989.042.01.19

Suthakorn, P. (1992). *The distribution of tin and associated minerals in Thailand. National conference on "geological resources of Thailand: Potential for future development"17-24 november 1992*. Bangkok, Thailand: Department of Mineral Resources.

Suwimonprecha, P. (1989). "Tin and niobium tantalum deposits associated with granites and pegmatites, Phuket, Thailand," (Germany: Tech. Univ. Aachen). Ph.D. thesis.

Sweetapple, M. T. (2000). *Characteristics of Sn-Ta-Be-Li industrial mineral deposits of the archaean pilbara craton, western Australia*. Australia: Australian Geological Survey Organization. Record 2000/44.

Tantiwanit, W., Raksaskulwong, L., and Mantajit, N. (1983). The upper paleozoic pebbly rocks in southern Thailand. Proceedings of the workshop on stratigraphic correlation of Thailand and Malaysia, technical paper. *Geol. Soc. Thail.* 1, 96–104.

Teng, J. X., and Gao, Y. B. (2019). *Investigation and exploration demonstration second-level project of the Fe, Pb and Zn Resource Base in the Western Kunlun area*. Xi'an,China: Xi'an Center of China Geological Survey Report, 526.

Tindle, A. G., and Breaks, F. W. (2000). Tantalum mineralogy of rare-element granitic pegmatites from the Separation Lake area, northwestern Ontario. Open File Report (Ontario Geological Survey) (6022). Sudbury, Canada: Ontario Geological Survey.

Tischendorf, G., Förster, H.-J., and Gottesmann, B. (2001). Minor- and trace-element composition of trioctahedral micas: A review. *Mineral. Mag.* 65, 249–276. doi:10.1180/002646101550244

Tischendorf, G., Gottesmann, B., Foerster, H.-J., and Trumbull, R. B. (1997). On Li-bearing micas; estimating Li from electron microprobe analyses and an improved diagram for graphical representation. *Mineral. Mag.* 61, 809–834. doi:10.1180/minmag.1997.061.409.05

Tukpho, T., and Fanka, A. (2021). Petrology and geochemistry of granitic rocks in dan chang area, suphan buri province, Central Thailand: Implication for petrogenesis. *SciAsia* 47, 609. doi:10.2306/scienceasia1513-1874.2021.066

Uchida, E., Endo, S., and Makino, M. (2007). Relationship between solidification depth of granitic rocks and formation of hydrothermal Ore deposits. *Resour. Geol.* 57, 47–56. doi:10.1111/j.1751-3928.2006.00004.x

Vladimirov, A. G., Lyakhov, N. Z., Zagorskiy, V. E., Makagon, V. M., Kuznetsova, L. G., Smirnov, S. Z., et al. (2012). Lithium deposits of spodumene pegmatites in siberia. *Chem. Sustain. Dev.* 20 (1), 3–20.

Wang, D., Dai, H., Liu, S., Wang, C., Yu, Y., Dai, J., et al. (2020). Research and exploration progress on lithium deposits in China. *China Geol.* 3, 137–152. doi:10.31035/cg2020018

Wang, H., Xu, Y. G., Yan, Q. H., and Zhan, X. Y. (2021). Research progress on Bailongshang pegmatite type lithium deposit, Xinjiang. *Acta Geol. Sin.* 95, 3085–3098.

Watkinson, I., Elders, C., Batt, G., Jourdan, F., Hall, R., and McNaughton, N. J. (2011). The timing of strike-slip shear along the Ranong and Khlong Marui faults, Thailand. *J. Geophys. Res.* 116, B09403. doi:10.1029/2011jb008379

Winter, J. D. (2001). *An introduction to igneous and metamorphic petrology*. Upper Saddle River, New Jersey: Prentice-Hall, 697.

Wu, F. Y., Liu, X. C., Liu, Z. C., Wang, R. C., Xie, L., Wang, J. M., et al. (2020). Highly fractionated Himalayan leucogranites and associated rare-metal mineralization. *Lithos* 352–353, 105319. doi:10.1016/j.lithos.2019.105319

Yao, J., Shu, L., Santosh, M., and Zhao, G. (2014). Neoproterozoic arc-Related mafic–ultramafic rocks and syn-collision granite from the Western segment of the jiangnan orogen, South China: Constraints on the neoproterozoic assembly of the yangtze and cathaysia blocks. *Precambrian Res.* 243, 39–62. doi:10.1016/j.precamres.2013.12.027

Yin, R., Han, L., Huang, X., Li, J., Li, W., and Chen, L. (2019). Textural and chemical variations of micas as indicators for tungsten mineralization: Evidence from highly evolved granites in the Dahutang tungsten deposit, South China. *Am. Mineral.* 104, 949–965. doi:10.2138/am-2019-6796

Zagorsky, V. Y., Vladimirov, A. G., Makagon, V. M., Kuznetsova, L. G., Smirnov, S. Z., D'yachkov, B. A., et al. (2014). Large fields of spodumene pegmatites in the settings of rifting and postcollisional shear–pull-apart dislocations of continental lithosphere. *Russ. Geol. Geophys.* 55 (2), 237–251. doi:10.1016/j.rgg.2014.01.008

Zaw, K., Meffre, S., Lai, C. K., Santosh, M., Burrett, C., Graham, I. T., et al. (2014). Tectonics and metallogeny of mainland Southeast Asia-a review and contribution. *Gondwana Res.* 26, 5–30. doi:10.1016/j.gr.2013.10.010

Zhang, X., Aldahri, T., Tan, X., Liu, W., Zhang, L., and Tang, S. (2020). Efficient co-extraction of lithium, rubidium, cesium and potassium from lepidolite by process intensification of chlorination roasting. *Chem. Eng. Process. process Intensif.* 147, 107777. doi:10.1016/j.cep.2019.107777

Zhao, F., Sun, Z., Xue, S., Li, G., Xia, Q., Hu, X., et al. (2022). Petrology and biotite geochemistry of Mengku granitoids in the Changning-Menglian suture zone, southwest China: Insights into magma evolution and Sn mineralization. *Ore Geol. Rev.* 145, 104879. doi:10.1016/j.oregeorev.2022.104879

Zhou, Z. X. (1986). The origin of intrusive mass in Fengshandong, Hubei province. *Acta Pet. Sin.* 2, 59–70.

Zimanovskaya, N. A., Oitseva, T. A., Khromykh, S. V., Travin, A. V., Bissatova, A. Y., Annikova, I. Y., et al. (2022). Geology, mineralogy, and age of Li-bearing pegmatites: Case study of tochka deposit (east Kazakhstan). *Minerals* 12 (12), 1478. doi:10.3390/min12121478